TUNNELING IN POLYMER QUANTIZATION AND QUANTUM ZENO EFFECT

A Thesis Submitted to
the Graduate School of Engineering and Sciences of
İzmir Institute of Technology
in Partial Fulfillment of the Requirements for the Degree of

MASTER OF SCIENCE

in Physics

by
Ozan SARGIN

July 2014
İZMİR

We approve the thesis of **Ozan SARGIN**

Examining Committee Members:

Prof. Dr. Durmuş Ali DEMİR
Department of Physics, İzmir Institute of Technology

Prof. Dr. R. Tuğrul SENGER
Department of Physics, İzmir Institute of Technology

Assist. Prof. Dr. Fatih ERMAN
Department of Mathematics, İzmir Institute of Technology

7 July 2014

Prof. Dr. Durmuş Ali DEMİR
Supervisor, Department of Physics
İzmir Institute of Technology

Prof. Dr. Nejat BULUT
Head of the Department of
Physics

Prof. Dr. R. Tuğrul SENGER
Dean of the Graduate School of
Engineering and Sciences

ACKNOWLEDGMENTS

I would like to express my appreciation to my supervisor Prof. Dr. Durmuş Ali DEMİR for his endless guidance, encouragement and outstanding support in this thesis. I feel fortunate to be able to benefit from his broad and deep knowledge and I am very grateful for his invaluable contribution to this work. I extend my warmest thanks to all my friends who were with me during not only the good times but also the bad times that I had to go through. Their friendship and support have always been important for me. Finally, my very special thanks go to my family and my one and only girlfriend G. for their never-ending love, support, patience and encouragement.

ABSTRACT

TUNNELING IN POLYMER QUANTIZATION AND QUANTUM ZENO EFFECT

Polymer quantization is a non-standard and exotic representation of the canonical commutation relations which is introduced in the context of loop quantum gravity to investigate the low energy limit of this non-perturbative quantization of gravity. It is one of the representations of the Weyl-Heisenberg algebra which is inequivalent to the standard Schrödinger representation. Since this representation is inequivalent to Schrödinger mechanics, by Stone-von Neuman uniqueness theorem there should not be a one to one correspondence between the operators of the two representations. It turns out that, one can not define the position and momentum operators simultaneously in this construction. In this work, we use the standard position operator and a second operator which is the analog of $\hat{p}$. To define an operator similar to the momentum operator $\hat{p}$, one needs to use a regularization length scale which can not be removed and stays as a free parameter in the theory. This free parameter is interpreted to descend from the fundamental discreteness of space in loop quantum gravity.

As another application of the polymer quantization scheme, in this work we investigate the one dimensional quantum mechanical tunneling phenomenon from the perspective of polymer representation of a non-relativistic point particle, derive the transmission and reflection coefficients and show that they add up to one which is the requirement of probability conservation. Since any tunneling phenomenon inevitably evokes a tunneling time we attempt an analytical calculation of tunneling times by defining an operator well suited in discrete spatial geometry. We expand our time expression in a Maclaurin series around zero polymer length scale and arrive at results which hint at appearance of the Quantum Zeno Effect in polymer framework. Quantum Zeno effect is the inhibition of a quantum system from making a transition from an initial state to a final state. And in summary, as a result of our work we can say that discretization of space leads to the Quantum Zeno effect.

ÖZET

POLİMER KUANTİZASYONUNDA TÜNELLEME ve KUANTUM ZENO ETKİSİ

Polimer kuantizasyonu gravitenin tedirgemesiz kuantizasyonunun düşük enerji limitlerini araştırmak için loop kuantum gravite bağlamında ortaya konmuş, kanonik komütasyon bağıntılarının standart dışı ve egzotik bir temsilidir. Bu, Weyl-Heisenberg cebirinin Schrödinger temsiline eşdeğer olmayan temsillerinden biridir. Bu temsil Schrödinger mekaniğine eşdeğer olmadığından, Stone-von Neuman özgünlük teoremine göre her iki temsilin operatörleri arasında birebir karşılıklılık olmamalıdır. Görülmüştür ki, bu yapıda konum ve momentum operatörleri aynı anda tanımlanamaz. Bu çalışmada biz standart konum operatörünün yanı sıra momentum operatörünün benzeri olan ikinci bir operatör kullanıyoruz. Momentum operatörüne benzer bir operatör tanımlamak için, teorinin serbest parametresi olarak kalıp kaldırılamayan düzenleyici bir uzunluk skalasına ihtiyaç vardır. Bu serbest parametrenin, loop kuantum gravitedeki uzayın temel parçalı yapısından kaynaklandığı düşünülür.

Polimer kuantizasyon planının bir başka uygulaması olarak, bu çalışmada biz bir boyutlu kuantum mekaniksel tünelleme olayını göreli olmayan bir parçacığın polimer temsili bakış açısıyla inceleyerek iletim ve yansıma katsayılarını çıkarıp bu katsayıların toplamının olasılık korunumunun gerektirdiği gibi bire eşit olduğunu gösteriyoruz. Herhangi bir tünelleme olayı kaçınılmaz olarak akıllara tünelleme zamanını getirdiğinden parçalı uzay geometrisine çok uygun bir zaman operatoru tanımlayarak analitik olarak tünelleme zamanı hesaplamaya girişiyoruz. Zaman ifademizi sıfır polimer uzunluk skalası etrafında Maclaurin serisine açarak Kuantum Zeno etkisinin polimer sisteminde varoluşuna işaret eden sonuçlara ulaşıyoruz. Kuantum Zeno etkisi bir kuantum sisteminin bir ilk durumdan son duruma geçiş yapmasını kısıtlamadır. Özet olarak, çalışmamızın sonucunda uzayın parçalı yapıya kavuşturulması Kuantum Zeno etkisine yol açar diyebiliriz.

TABLE OF CONTENTS

APPENDICES

LIST OF FIGURES

Figure **Page**

CHAPTER 1

INTRODUCTION

Quantizing gravity is probably the most challenging problem confronting today's theoretical physicists. Loop Quantum Gravity (LQG) is one of the formalisms pursued by physicists to reach this goal, and it has been quite successful in incorporating the background independent character demanded by general relativity. However, deep conceptual and practical differences between the background independent description and low energy description make it difficult to show that the former turns into the low energy description smoothly.[1] That's exactly where the Polymer quantization comes into play. Polymer representation is a quantization scheme which is a low energy limit of LQG. It is a program initiated to inspect and resolve some conceptual problems in LQG in toy model settings.

Polymer quantization approach has been used to study the features arising in loop quantum gravity [2, 3] and especially loop quantum cosmology (LQC) [4, 5] since polymer framework and LQC have the same configuration space [6]. This quantization scheme has been applied to toy models such as a free particle in one dimension [2] and simple harmonic oscillator [2, 7, 8]. [2] Galilean symmetries have been investigated [9], continuum limit of polymer quantum systems has been explored [10, 11], singular potentials such as $1/r$ [12] and $1/r^2$ [13] have been studied and it has been shown that polymer quantization leads to a modified uncertainty principle [14]. Furthermore, statistical thermodynamics of a solid and ideal gas have been studied in [15] and Bose-Einstein condensation has been investigated in [16]. Entropies in the polymer and standard Schrödinger hilbert spaces are analysed and they are shown to converge in the limit of vanishing polymer scale [17].

Tunneling is a purely quantum phenomenon that is caused by the uncertainty principle. Inspired by the fact that uncertainty principle gets modified in the framework of polymer quantum mechanics [14]; in this work we study the tunneling of a non-relativistic quantum particle through a rectangular barrier in polymer quantization. The reason why we choose a rectangular barrier is that, one can decompose any type of potential into infinitesimal rectangular potential barriers.

[1] See [1] for an analysis in this direction.

[2] [8] stands out of the previous works on harmonic oscillator in that it conveys that the spectrum of the oscillator consists of bands similar to periodic potentials.

Tunneling time is the phenomenon that inevitably comes to one's mind along with tunneling. It has been bothering physicists for decades since the works of Condon in 1930 [18] and MacColl in 1932 [19] for reasons that time is not represented by an operator in quantum mechanics [20] and classically tunneling time is imaginary [21]. Hence, we embark on calculating tunneling times by defining a time operator which is odd when we consider the fact that time is just a parameter in quantum mechanics without an operator counterpart.

The next concept that we consider in this work is the relation of this tunneling time to the Quantum Zeno Effect (**QZE**). QZE is a phenomenon which gathers a lot of interest among physicists and general public alike simply because it gives the impression that time can be stopped. In this thesis, we will not dwell too deeply on the details of QZE since there is a good deal of literature out there that may be consulted such as [22–29]. QZE may be defined simply as the inhibition of a quantum system's time evolution by frequent measurements of the system's state. This means that by frequent measurements you restrain the system from making a transition from an initial state to a final state and in a sense , in the limit of infinitely many measurements in a finite time interval, the system's evolution is confined in a small subspace of the Hilbert space. The principle idea that led Misra and Sudarshan in [30] to predict the viability of the Quantum Zeno Effect is that unstable quantum systems were expected to exhibit a short-time non-exponential decay law. It was realized that, contrary to the classical heuristic exponential decay law, quantum systems follow three distinct decay phases. The short-time phase is a quadratic one, the intermediate phase is the exponential decay and the long-time phase follows a power law. Misra and Sudarshan proposed that if frequent measurements are made in the short-time phase of the decay and if these measurements are ideal in the sense that they are von Neumann measurements which are represented by one-dimensional projectors; after each measurement the state of the system is projected back to the initial state, as a result time evolution of the system is slowed down and eventually comes to a halt. In recent years, it has been predicted that one may observe an increase in the decay rates of unstable systems as a result of frequent measurements if the frequency of observations is properly adjusted and in literature this phenomenon is referred to as the Quantum Anti-Zeno Effect (**AZE**) [31, 32]. The validity of Quantum Zeno and anti-Zeno effects are now both established. Experimental evidence for the non-exponential decay in quantum tunneling was reported in [33], AZE and QZE are experimentally confirmed in works like [34–38]. In [39] Quantum Zeno and anti-Zeno effects are simultaneously reported to be observed.

In works on QZE and AZE, it is stated that decay rates depend on the frequency of

the measurements made on the system [40]. If the frequency of the observations is such that you measure the system's state each and every time in the short-time phase of the decay then the decay rate drops; on the contrary, if the measurement frequency is such that you observe the system right at the point where the decay rate changes character , i.e. the point where the short-time phase gives way to the exponential phase, the decay accelerates.

Following this lead, we analyse our tunneling time expression to discover the fingerprints of QZE and AZE. In our work, the parameter that effectively plays the role of frequency of measurements is the polymer length scale. Altering this free parameter of the theory we examine the change in tunneling times.

This work consists of three main parts. In the first, a review of the polymer particle representation is given. In the second, tunneling problem is analyzed in both the Schrödinger and the polymer particle schemes. Finally, in the last part, we consider tunneling times and arrive at rather interesting results regarding the validity of the Quantum Zeno effect in the framework of polymer quantization.

1.1. Review of the Polymer Particle Description

In this section, we give a brief outline of the formulation and the notations of the polymer particle description; the details can be found in [2]. The system under consideration is a non-relativistic particle moving on the real line $\mathbb{R}$.

1.1.1. Weyl-Heisenberg Algebra

According to Dirac's procedure, the first step in constructing a quantum theory from a classical one is to define a quantization rule or algebra that replaces the Poisson bracket of observables by the commutator of the operators which are the counterparts of observables in the quantum theory. The classical particle is the simplest physical system whose states are defined through the algebra obtained as the sup-norm closure of the polynomial algebra generated by position and momentum. Following the Dirac procedure, the quantum particle is defined by an algebra of observables generated by position and momentum operators which satisfy the Heisenberg canonical commutation relations

$$[\hat{x}, \hat{p}] = i\hbar, \qquad [\hat{x}, \hat{x}] = 0, \qquad [\hat{p}, \hat{p}] = 0;$$

where we have considered one spatial dimension for simplicity. The canonical commutation relations given above imply that position and momentum can not be self-adjoint elements of a C*-algebra, since they can not be given a finite norm. In order to overcome this technical difficulty, a solution is put forward by Weyl, which involves the use of a polynomial algebra generated by the exponentiated position and momentum operators. This algebra is called the Weyl-Heisenberg algebra since the group associated to this algebra is the Heisenberg Lie group.

In Weyl-Heisenberg algebra [41], one associates a Weyl operator $\hat{W}(\zeta)$ (which will turn out to be the product of exponentiated position and momentum operators) to each complex number ζ and in return $\hat{W}(\zeta)$ generates a vector space **W**. A product, called the Weyl relation, is introduced on **W** via:

$$\hat{W}(\zeta_1)\hat{W}(\zeta_2) = e^{\frac{i}{2}Im(\zeta_1\bar{\zeta_2})}\hat{W}(\zeta_1 + \zeta_2) \tag{1.1}$$

and an involution to ensure the unitarity of operators via:

$$\hat{W}^*(\zeta) = \hat{W}(-\zeta). \tag{1.2}$$

Generally, physicists introduce a length scale *d* and split $\hat{W}(\zeta)$ as follows [3] :

$$\hat{W}(\zeta) = e^{\frac{i}{2}\lambda\mu}\hat{U}(\lambda)\hat{V}(\mu) \tag{1.3}$$

where

$$\zeta = \lambda d + i\,\tfrac{\mu}{d}\ ;\ \hat{U}(\lambda) \equiv \hat{W}(\lambda \mathrm{d}) \text{ and}$$
$$\hat{V}(\mu) \equiv \hat{W}(i\,\tfrac{\mu}{d}).$$

The one parameter unitary operators $\hat{U}(\lambda)$ and $\hat{V}(\mu)$ satisfy the following relations,

- $\hat{U}(\lambda_1)\hat{U}(\lambda_2) = \hat{U}(\lambda_1 + \lambda_2)$
- $\hat{V}(\lambda_1)\hat{V}(\lambda_2) = \hat{V}(\lambda_1 + \lambda_2)$
- $\hat{U}(\lambda)\hat{V}(\mu) = e^{-i\lambda\mu}\,\hat{V}(\mu)\hat{U}(\lambda)$

which are called the Weyl commutation relations[3] and represent the form taken by the Heisenberg commutation relations in terms of Weyl operators $\hat{U}(\lambda)$ and $\hat{V}(\mu)$.

[3] Please refer to Appendix A.1 for the derivation.

1.1.2. The Schrödinger Representation

According to the von Neuman uniqueness theorem [42], all the regular irreducible representations of **W** are unitarily equivalent to the standard Schrödinger representation. The regularity condition is an extremely mild request and is standard in the theory of representations of Lie algebras. The regularity condition reads as follows. A representation of the Weyl-Heisenberg algebra is regular if the representations of the unitary operators $\hat{U}(\lambda)$ and $\hat{V}(\mu)$ are strongly continuous in λ and μ respectively.

For unitary operators in a Hilbert space, strong continuity is equivalent to the weaker condition of weak continuity. In the case of separable spaces, weak continuity is in turn equivalent to the property that the matrix elements of the one parameter unitary operators $\hat{U}(\lambda)$ and $\hat{V}(\mu)$ are Lebesgue measurable functions. This is a manifestation of how reasonable the regularity condition is.

In light of all these, $\hat{W}(\zeta)$ is represented via:

$$\hat{W}(\zeta)\psi(\underline{x}) = e^{\frac{i}{2}\alpha\beta}e^{i\alpha\underline{x}}\psi(\underline{x}+\beta) \tag{1.4}$$

where $\zeta = \alpha + i\beta$. This implies that

$$\hat{U}(\lambda)\psi(x) = e^{i\lambda x}\psi(x); \tag{1.5}$$

$$\hat{V}(\mu)\psi(x) = \psi(x+\mu) \tag{1.6}$$

for all $\psi \in \mathrm{H}_{Sch}$.

By Stone's theorem on one parameter groups of strongly continuous unitary operators, regularity is equivalent to the existence of the generators of the Weyl operators, namely $\hat{x}$ and $\hat{p}$, as self-adjoint unbounded operators in H. Furthermore, one can show that they have a common invariant dense domain. Thus, regularity allows to reconstruct the Heisenberg algebra from the Weyl algebra.

The one parameter unitary groups $\hat{U}(\lambda)$ and $\hat{V}(\mu)$ are weakly continuous in the parameters λ and μ. This ensures that there exist self-adjoint operators $\hat{x}$ and $\hat{p}$ on H_{Sch} such that

$$\hat{U}(\lambda) := e^{i\lambda\hat{x}}, \tag{1.7}$$

$$\hat{V}(\mu) := e^{\frac{i\mu}{\hbar}\hat{p}}. \tag{1.8}$$

The Hilbert space of Schrödinger representation is $\mathrm{H}_{Sch} = \mathrm{L}^2(\mathbb{R}^s, d^s x)$, where $\mathrm{s} =$ space dimension.

In terms of momentum wave functions $\psi(k)$, we have

$$\hat{U}(\lambda)\psi(k) = \psi(k-\lambda); \tag{1.9}$$

$$\hat{V}(\mu)\psi(k) = e^{i\mu k}\psi(k). \tag{1.10}$$

It is obvious that $\hat{U}(\lambda)$ and $\hat{V}(\mu)$ are unitary operators in H_{Sch} and that they define a strongly continuous representation of the Weyl C*-algebra :

$$\begin{aligned} \hat{U}(\lambda)\hat{V}(\mu)\psi(x) &= e^{i\lambda x}\psi(x+\mu), \\ \hat{V}(\mu)\hat{U}(\lambda)\psi(x) &= e^{i\lambda(x+\mu)}\psi(x+\mu), \\ \hat{U}(\lambda)\hat{U}(\mu)\psi(x) &= \hat{U}(\lambda+\mu)\psi(x), \\ \hat{V}(\lambda)\hat{V}(\mu)\psi(x) &= \hat{V}(\lambda+\mu)\psi(x). \end{aligned} \tag{1.11}$$

1.1.3. The Polymer Particle Representation

The Schrödinger representation is the only irreducible representation of the Weyl algebra in which the Weyl operators $\hat{U}(\lambda)$ and $\hat{V}(\mu)$ are continuous functions of λ and μ with respect to weak operator topology.

There are many irreducible representations where this condition on weak continuity is not met. One example of these representations is the Polymer representation. In this construction the operator $\hat{V}(\mu)$ is not weakly continuous in the parameter μ due to the discrete structure assigned to the space; hence there does not exist a one to one correspondence between $\hat{V}(\mu)$ and a self-adjoint operator $\hat{p}$ such that $\hat{V}(\mu) = \exp[\frac{i\mu}{\hbar}\hat{p}]$. [4]

The next step in the quantization is to find a concrete Hilbert space. The central difference between Schrödinger and polymer quantization is the choice of a non-seperable Hilbert space H_{poly}. The polymeric Hilbert space is constructed as follows: First, a graph γ is chosen so that it consists of a countable set $\{x_i\}$ of points on the real line without accumulation points. Next, we denote by Cyl_γ the vector space of complex valued cylindrical

[4] See [43], which analyzes the non-existence of the momentum operator in a context where Bohr's complementarity principle is equivalent to the existence of representations of CCRs.

functions $f(k)$ of the type

$$f(k) = \sum_j f_j \exp[-ix_j k] \tag{1.12}$$

on $\mathbb{R}$, where x_j are real and f_j are complex numbers with a suitable fall off. The functions $f(k)$ are said to be cylindrical with respect to a graph γ. If we consider all possible graphs γ, where the number and locations of the points can vary from one graph to another, then Cyl=$\bigcup_\gamma Cyl_\gamma$ is the infinite dimensional vector space of functions cylindrical with respect to some graph γ. Then, we introduce a Hermitian inner product on Cyl by demanding that the basis elements $\exp[-ix_j k]$ are orthonormal:

$$\langle e^{-i\vec{x_i}.\vec{k}} | e^{-i\vec{x_j}.\vec{k}} \rangle = \delta_{\vec{x_i},\vec{x_j}}.$$

The polymer particle Hilbert space H_{poly} of the polymer representation is the Cauchy completion of Cyl with respect to the inner product defined above and it can compactly be written as $H_{poly} = L^2(\mathbb{R}_d, d_{\mu_d})$ with d_{μ_d} the corresponding Haar measure and $\mathbb{R}_d$ the real line endowed with discrete topology. H_{poly} consists of functions Ψ on the real line which vanish up to a countable subset and satisfy the condition

$$\sum_{x\in\mathbb{R}} |\Psi(x)|^2 < \infty, \tag{1.13}$$

and the scalar product defined by

$$(\Psi, \Phi) = \sum_{x\in\mathbb{R}} \overline{\Psi(x)}\Phi(x) \ . \tag{1.14}$$

The Weyl-Heisenberg algebra on H_{poly} is represented in the same way as in the Schrödinger representation.

$$\hat{W}(\zeta) f(k) = e^{\frac{i}{2}\lambda\mu} \hat{U}(\lambda)\hat{V}(\mu) f(k) \tag{1.15}$$

where ζ = α+$i\beta$ and the action of $\hat{U}(\lambda)$ and $\hat{V}(\mu)$ is given by:

$$\hat{U}(\lambda) f(k) = f(k-\lambda), \tag{1.16}$$

$$\hat{V}(\mu) f(k) = e^{i\mu k} f(k). \tag{1.17}$$

If we associate a ket $|x_j\rangle$ with the basis elements $\exp[-ix_j k]$ we can express $\exp[-ix_j k]$ as a generalized scalar product $(k, x_j) = e^{-ix_j k}$. Then $|x_j\rangle$ is an orthonormal basis and the action of $\hat{U}(\lambda)$ and $\hat{V}(\mu)$ is given by

$$\hat{U}(\lambda)|x_j\rangle = e^{i\lambda x_j}|x_j\rangle, \tag{1.18}$$

$$\hat{V}(\mu)|x_j\rangle = |x_j - \mu\rangle. \tag{1.19}$$

$\hat{U}(\lambda)$ is weakly continuous in λ whence there exists a self-adjoint operator $\hat{x}$ on H_{poly} with $\hat{U}(\lambda)$= $\exp[i\lambda\hat{x}]$. Its action can be expressed as $\hat{x}|x_j\rangle = x_j|x_j\rangle$. However, $\hat{V}(\mu)$ fails to be weakly continuous in μ because no matter how small μ is, $\hat{V}(\mu)|x_j\rangle$ and $|x_j\rangle$ are orthogonal to one another, i.e.

$$\lim_{\mu\to 0}\langle x_j|\hat{V}(\mu)|x_j\rangle = 0 \text{ while } \hat{V}(\mu=0) = 1 \text{ and } \langle x_j|x_j\rangle = 1.$$

Thus there is <u>no</u> self-adjoint operator $\hat{p}$ on H_{poly} satisfying $\hat{V}(\mu) = \exp[i\frac{\mu}{\hbar}\hat{p}]$. Since there does not exist a momentum operator, position $\hat{x}$ and the translation operator $\hat{V}(\mu)$ are the main operators that are used in the construction of the polymer representation. These two operators satisfy the commutation [5]:

$$[\hat{x}, \hat{V}(\mu)] = -\mu\hat{V}(\mu). \tag{1.20}$$

We now discuss the dynamics of Polymer representation:

The analog of the Schrödinger momentum operator is defined in this construction as $\hat{p} = \hbar\hat{K}_{\mu_0}$, where $\hat{K}_{\mu_0} = \frac{\hat{V}(-\mu_0)-\hat{V}(\mu_0)}{-2i\mu_0}$.[6] The generic classical Hamiltonian is of the form $H = \frac{p^2}{2m} + W(x)$.

Since $\hat{x}$ is well-defined, the main problem is that of defining the operator analog of $\hat{p}^2$ and thereby regularizing the Hamiltonian. For this purpose, we use the definition $\hat{p} = \hbar\hat{K}_{\mu_0}$ and obtain the Hamiltonian in terms of $\hat{K}_{\mu_0}$ as

$$\hat{H}_{\mu_0} = \frac{\hbar^2}{2m}\hat{K}^2_{\mu_0} + \hat{W}(\hat{x}) \tag{1.21}$$

then we calculate the square of $\hat{K}_{\mu_0}$

$$\hat{K}^2_{\mu} = -\frac{1}{4\mu^2}\left[\hat{V}(\mu) - \hat{V}(-\mu)\right]\left[\hat{V}(\mu) - \hat{V}(-\mu)\right] \tag{1.22}$$

using the additivity property of the translation operator we get

$$\hat{K}^2_{\mu} \;=\; -\frac{1}{4\mu^2}\left[\hat{V}(2\mu) - \hat{V}(0) - \hat{V}(0) + \hat{V}(-2\mu)\right] \tag{1.23}$$

and then we obtain

$$\hat{K}^2_{\mu} = \frac{1}{4\mu^2}\left[2 - \hat{V}(2\mu) - \hat{V}(-2\mu)\right] \tag{1.24}$$

then we make the change $2\mu \to \mu_0$ and get the result

$$\hat{K}^2_{\mu_0} = \frac{1}{\mu_0^2}\left[2 - \hat{V}(\mu_0) - \hat{V}(-\mu_0)\right]. \tag{1.25}$$

[5] Please refer to Appendix A.1 for the derivation.
[6] Please refer to Appendix A.1 for the derivation.

The square of the momentum operator can alternatively be calculated directly from the approximation

$$e^{\frac{i\mu_0\hat{p}}{\hbar}} + e^{\frac{-i\mu_0\hat{p}}{\hbar}} \approx 2 - \frac{\mu_0^2\hat{p}^2}{\hbar^2}, \qquad for \quad \hat{p} \ll \frac{\hbar}{\mu_0}. \tag{1.26}$$

Replacing the exponentials directly by the translation operators $\hat{V}(\mu_0)$ and $\hat{V}(-\mu_0)$ respectively we obtain

$$\hat{p}^2 = \frac{\hbar^2}{\mu_0^2}\left[2 - \hat{V}(\mu_0) - \hat{V}(-\mu_0)\right]. \tag{1.27}$$

After all these (1.21) takes the form:

$$\hat{H}_{\mu_0} = \frac{\hbar^2}{2m\mu_0^2}\left[2 - \hat{V}(\mu_0) - \hat{V}(-\mu_0)\right] + \hat{W}(\hat{x}). \tag{1.28}$$

The energy eigenvalue problem $\hat{H}_{\mu_0}\psi = E\psi$ takes the form of a second order difference equation in the position representation:

$$\psi(x+\mu_0) + \psi(x-\mu_0) = \left[2 \quad - \quad \frac{2m\mu_0^2}{\hbar^2}(E - W(x))\right]\psi(x) \tag{1.29}$$

as follows from (1.19). [7]

[7] See [44] for details.

CHAPTER 2

TUNNELING IN SCHRÖDINGER AND POLYMER SCHEMES

2.1. A Brief History of Tunneling

Tunneling is one of the most mysterious phenomena of quantum mechanics but at the same time it is such a basic and important process that it occurs in all quantum systems in nature from the nucleo-synthesis in stars down to the evolution of the early universe. In one sentence we can define tunnel effect as the penetration of matter waves and the transmission of particles through a classically forbidden region of space, viz a high potential barrier. From the very beginning quantum tunneling has remained a hot topic with a host of applications and been a fertile research ground considering the number of Nobel prizes in physics awarded for tunneling related works.

Louis de Broglie's introduction , in 1923, of the fundamental hypothesis that matter may be endowed with a dualistic nature, namely particles may also have the characteristics of waves led to two different inspirations. The first was the realization that, in analogy with light waves, matter waves presumably would also penetrate and be transmitted through classically forbidden regions. The second was the invention of the Schrödinger's wave equation, whereby a particle is assumed to be represented by a solution to this equation, to wit the wave function. The continuous nonzero nature of the wave functions, even in regions where the kinetic energy becomes negative, implies an ability to penetrate through such regions and a probability of tunneling from one classically allowed region to another. Let us elaborate on that first inspiration a little more.

According to de Broglie's hypothesis a particle has a wavelength inversely proportional to its velocity. This implies that a particle of energy E incident on a region of potential energy V enters a medium of index of refraction

$$n = \sqrt{\frac{E-V}{E}} \, . \tag{2.1}$$

Under normal circumstances, when the energy of the particle is greater than the potential, so that the index of refraction is real, the medium is dispersive and classically al-

lowed, but in classically forbidden regions where the particle's total energy is less than the potential, i.e. $E < V$, the kinetic energy of the particle becomes negative and at the same time the index of refraction defined above turns in to an imaginary number. We have an analogous situation in optics, viz the penetration of light through a thin reflecting metallic layer signals an imaginary index of refraction.

A similar phenomenon is observed in total internal reflection in optics. During total internal reflection, at the interface of two transparent media there appears an evanescent light wave which can not be accounted for using geometric optics. In the less dense medium, the normal component of the propagation vector is imaginary and the amplitude of the wave decreases exponentially rather than displaying an oscillatory behaviour. If a second medium of index of refraction higher than the first one is within reach of this evanescent wave, an attenuated part of the incident wave can be transmitted and this whole process is termed frustrated total internal reflection in literature.

Making an analogy with frustrated total internal reflection, physicists expected to observe a similar barrier penetration process for matter waves but a quantitative analysis of this tunneling effect had to await Schrödinger's wave equation and Max Born's probabilistic interpretation of the solutions to this equation.

Shortly after the advent of Schrödinger's wave equation, Friedrich Hund was the first to use quantum mechanical tunneling in explaining the theory of molecular spectra in a series of papers in 1927. The first paper of this series deals with the splitting of the ground state of a molecule. An outer electron moving in an atomic potential with two or more minima separated by classically impenetrable barriers was the case that tunneling was applied to by Hund. He was primarily concerned with characterizing the electronic energy eigenfunctions in terms of the quantum numbers of the system for the limiting cases of bounded and widely separated atoms. By means of tunneling he explained the sharing of an electron between the atoms of the molecule represented by potential wells and made the distinction between classical and quantum orbits, i.e. he discussed the basics of covalent binding. In the third paper of the series, Hund discussed the superposition of ground states of a molecule and showed that tunneling is the reason for the non-stationary character of this superposed state. Building on his first paper, he realized the omnipresence of reflection symmetric potentials with classically impenetrable barriers. The stationary states of these potentials are either odd or even functions of the relative coordinates of the constituent atoms. The superposed state composed of an even ground state and odd first excited state is non-stationary by character and oscillates back and forth between the classical equilibrium positions. In this paper,

Hund calculated also the reciprocal tunneling rate and showed that transitions between chiral isomers are improbable for biological molecules.

Hund's work was related to tunneling between bound states. Tunneling between unbound states with continuum energy eigenvalues was first considered by Lothar Nordheim in 1927. In his work Nordheim discussed the thermionic emission of electrons from a heated metal and reflection of electrons from metal surfaces. Utilizing Arnold Sommerfeld's electron theory of metals and modeling the surface of the metal which confines the electrons as a steep potential rise, he calculated the wave function and discovered that for particle energies near the top of the barrier there is a finite probability of either transmission through the barrier or reflection, although classically there would be only one or the other. For rectangular potential barriers, he noted that an electron whose energy is insufficient to go over the barrier classically can still tunnel through it quantum mechanically, whereas classically it will always be reflected back. Although he realized the possibility of tunneling, at the end of his calculations Nordheim thought that tunneling would be of little physical significance because the transmission coefficients he got was very small unless the barrier is a few atoms thick. With this work Nordheim extended the case of tunneling between bound states first noticed by Hund to the case of tunneling between continuum states.

In 1928, physicists believed that tunneling could occur if the barrier is distorted by application of an external electric field. Oppenheimer was the first to examine this situation in the case of the electron in a hydrogen atom exposed to a high uniform electric field. He used Dirac's bra-ket notation and time dependent perturbation theory to calculate the matrix elements between discrete energy eigenstates of the unperturbed hydrogen atom and the continuum energy states of the electron in a uniform field. He observed that even if the total energy is less than the potential, the matrix elements are non-zero; for the there is an overlap of wave functions in classically forbidden regions. As a continuation of this work he submitted an analysis of Millikan's experiments on field emission from cold metals to the National Academy of Sciences on March 28 of the same year. But both of his works were criticized since he used linearly dependent unperturbed energy eigenfunctions in the expansion of the wave function of the system; so interpretation of expansion coefficients as probability amplitudes is questionable.

Although Oppenheimer's discussion of cold emission was three dimensional and physically sophisticated, because of the questionable interpretation of probability amplitudes, Fowler and Nordheim decided to attack the same problem *de novo*. They based their treatment on a one-dimensional triangular barrier model of the surface of the metal and con-

sidered a uniform electric field applied perpendicular to the surface plane of the metal. In this work they made a rigorous analysis of the dependence of the cold-emission current on the external field strength and the work function of the metal.

Another application of tunneling in those years came with the theories on alpha decay. The theory of alpha radioactivity based on quantum tunneling was first proposed by Gamow. After reading the paper of Ernest Rutherford about the puzzle surrounding Geiger's 1921 experiments on scattering alpha particles from uranium, Gamow immediately saw the opportunity to apply the newly born quantum theory of tunneling to this phenomenon to explain the enormous range of decay rates and more importantly the possibility of emission for alpha particles whose energy is less than the Coulomb barrier of the uranium nucleus.

During his scattering experiments with alpha particles from radioactive polonium-212, Geiger confirmed the presence of the repulsive Coulomb potential in uranium up to a height of at least $8.57MeV$. But in the mean time it was also known that uranium-238 emits alpha particles with energies less than half of this potential energy value. This posed a serious conundrum for physicists if the alpha particles were to be assumed to pass over the top of the Coulomb potential profile for emission into continuum. A lot of unsuccessful attempts were made before Gamow attacked the same problem. Gamow decided to take up this puzzle after he arrived at Göttingen from the Soviet Union. His first attempt was a failure because in that he assumed that the alpha particle is a point particle located in the Coulomb field of the nucleus. He found a continuous spectrum for the emitted alpha particle energies and this was in contrast with the empirical fact that there are certain characteristic energies with which the particles are emitted. Later Gamow thought of combining the attractive nuclear forces with the repulsive Coulomb force to get an effective barrier for the alpha particle to tunnel through. He solved the Schrödinger equation with this potential and imposed the outgoing wave boundary condition. The outcome of this calculation revealed that this boundary value problem does not have a solution for real energies but for complex energies it does. Interpreting the complex part of the energy as the decay width he obtained the Geiger-Nuttel formula which relates the decay width with the emitted particle energies.

A day after Gamow's submission, Gurney and Condon submitted their paper on alpha decay to Nature also utilizing quantum mechanical tunneling. They published a longer exposition of this work in The Physical Review in February 1929. During their work Gurney and Condon realized that it is not essential to know the explicit form of the potential inside the nucleus, they only had to assume that it becomes zero at a distance of nuclear radius. Using the WKB approximation they found the solution to the Schrödinger equation for the

radial part of the wave function with the condition that the amplitude of it must be large inside and small outside the nucleus. From this solution they obtained the decay width and the energy of the emitted alpha particle.

The common factor in all these quantum mechanical theories were that they could account for two important features of the alpha decay easily. First, because quantum mechanics is intrinsically probabilistic it was easy to understand the statistical character of alpha decay with its constant transition rate and exponential decay. Second, the theories could account for the functional relationship between the rate of decay and particle emission energies and they yielded results that were in semi-quantitative agreement with the experiments.

After the second Wold War, the quantum mechanical tunneling evolution continued with discovery of various tunneling phenomena and invention of various devices based on tunneling such as tunneling diode of Esaki (1957) and Josephson junctions (1962).

2.2. Tunneling and the Uncertainty Principle

We will devote this section to an investigation as to why tunneling is exclusively a quantum phenomenon and does not have a counterpart in classical physics. On the face of it, tunneling of a particle through a barrier looks like a paradoxical problem, since if the height of the potential barrier is greater than the total energy of the particle

$$E = \frac{p^2}{2m} + V(x) \tag{2.2}$$

then inside the barrier region the kinetic energy of the particle, i.e. the first term in (2.2), is negative and momentum p is imaginary; but being an observable, momentum must be real. Our way of thinking in terms of classical physics is at the root of this apparent paradox. We naively assume that at each instant of particle's motion we know the kinetic and potential energies of the particle simultaneously and separately. This amounts to being able to assign values to the position and momentum of the particle at the same time but this is a direct violation of the uncertainty principle.

If we determine the position of the particle inside the barrier, according to the uncertainty principle its momentum is uncertain by an amount $\sqrt{\overline{(\Delta p)^2}}$. Thus if we know the coordinate of the particle to be x, then its total energy cannot be E. Since the probability of tunneling through the barrier is proportional to

$$exp\left[-\frac{2}{\hbar}\int_0^L \sqrt{2m\{V(x)-E\}}\,dx\right], \tag{2.3}$$

if there is a significant chance for the particle to tunnel we should have

$$2\sqrt{2m(V_{max} - E)}L \approx \hbar \ . \tag{2.4}$$

Applying the uncertainty principle and noting the fact that in order to locate the particle inside the barrier the uncertainty in position should be less than the barrier width , we get the uncertainty in momentum to be

$$\overline{(\Delta p)^2} = \frac{\hbar^2}{4(\Delta x)^2} = \frac{\hbar^2}{4L^2} \ . \tag{2.5}$$

Substituting L from (2.4) we find

$$\frac{\overline{(\Delta p)^2}}{2m} = V_{max} - E \ . \tag{2.6}$$

What this means is that, inside the barrier a local kinetic energy of at least the difference between the height of the barrier and the total energy of the particle is provided to the particle by the uncertainty principle.

All these arguments give us enough evidence to claim that tunneling is a quantum phenomenon.

2.3. Tunneling in Schrödinger Representation

In this section we will investigate the tunneling problem in the Schrödinger representation. This is a rather basic problem that is treated in almost any introductory text book in quantum mechanics such as [45, 46]. The reason that we include it in this work is that we want the reader to see the similarities and differences between the two inequivalent representations of the Weyl-Heisenberg algebra in a concrete example.

Consider the motion of a particle in a potential which has the form of the rectangular barrier shown in Figure 2.1. According to classical mechanics a particle incident upon this barrier from the left with total energy E less than V_0 would always be reflected back. Classically no particle can penetrate the barrier because inside the barrier it would have a negative kinetic energy. However, quantum mechanical treatment of this problem leads to the conclusion that both reflection and transmission are possible with a non-vanishing probability.

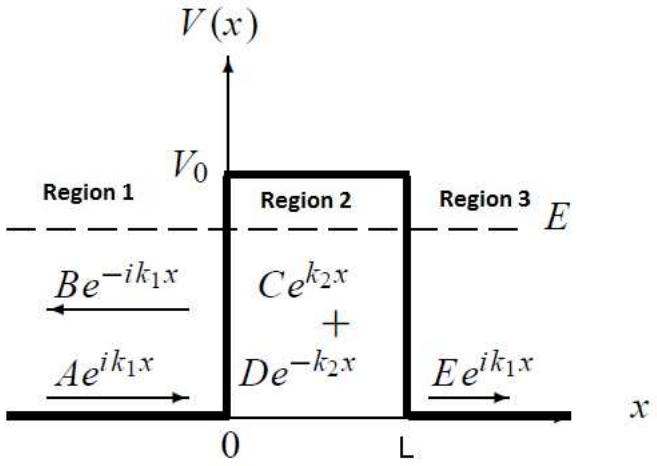

Figure 2.1. Potential profile and propagation directions of the incident, reflected and transmitted waves. *This figure is from [45] with a couple of additions.*

We analyse this problem by dividing the potential into three distinct regions and solving the relevant eigen-value equations pertaining to these regions.

2.3.1. Region 1:

In this region the particle is free because the problem we are studying is essentially a one-dimensional scattering problem in which a particle interacts with a potential in a given interval, i.e. inside the barrier. Therefore, the Hamiltonian is the free particle one and the eigen-value equation reads

$$-\frac{\hbar^2}{2m}\frac{d^2\psi_1}{dx^2} = E\psi_1. \tag{2.7}$$

This equation can be rewritten as

$$\frac{d^2\psi_1}{dx^2} + k_1^2\psi_1 = 0 \tag{2.8}$$

where we have made the definition $k_1^2 = \frac{2mE}{\hbar^2}$. The solution of this second order differential equation is

$$\psi_1(x) = Ae^{ik_1x} + Be^{-ik_1x} \tag{2.9}$$

where A and B are the amplitudes of incident and reflected waves but they are undetermined coefficients for now.

2.3.2. Region 2:

Since this is the barrier interval, the Hamiltonian of the particle has an additional potential term here.

$$\hat{H} = \frac{\hat{p}^2}{2m} + \hat{V}_0. \tag{2.10}$$

The corresponding eigen-value equation is

$$-\frac{\hbar^2}{2m}\frac{d^2\psi_2}{dx^2} + V_0\psi_2 = E\psi_2. \tag{2.11}$$

(2.11) can be rewritten as

$$\frac{d^2\psi_2}{dx^2} - \frac{2m(V_0 - E)}{\hbar^2}\psi_2 = 0. \tag{2.12}$$

Making the definition $k_2^2 = \frac{2m(V_0-E)}{\hbar^2}$, we have

$$\frac{d^2\psi_2}{dx^2} - k_2^2\psi_2 = 0. \tag{2.13}$$

The solution of (2.13) is

$$\psi_2(x) = Ce^{k_2x} + De^{-k_2x}. \tag{2.14}$$

As you can see the wave function in this region has an exponential decay character rather than an oscillatory behaviour.

2.3.3. Region 3:

The Hamiltonian in this region is also the free particle Hamiltonian as for $x < 0$. The eigen-value equation is the same as (2.7) but here the time-independent Schrödinger equation does not have the reflected wave solution because there is nothing at large positive values of x to cause a reflection. Hence the wave function in this region is

$$\psi_3(x) = Ee^{ik_1 x}. \tag{2.15}$$

2.3.4. Transmission and Reflection Coefficients

Combining the three regions the total wave function of the particle can be written as

$$\psi(x) = \begin{cases} \psi_1(x) = Ae^{ik_1 x} + Be^{-ik_1 x}, & x \leq 0 \\ \psi_2(x) = Ce^{k_2 x} + De^{-k_2 x}, & 0 < x < L \\ \psi_3(x) = Ee^{ik_1 x}, & x \geq L. \end{cases}$$

The reflection and transmission coefficients are defined as

$$R = \frac{|B|^2}{|A|^2}, \qquad T = \frac{|E|^2}{|A|^2}\,. \tag{2.16}$$

Using the continuity conditions for the wave function and its derivatives at the boundaries we calculate the transmission and reflection coefficients. For the first boundary, i.e. $x = 0$, we have

$$\psi_1(0) = \psi_2(0), \tag{2.17}$$

which gives

$$A + B = C + D. \tag{2.18}$$

Equating the derivatives at $x = 0$

$$\dot{\psi}_1(0) = \dot{\psi}_2(0), \tag{2.19}$$

which leads to

$$ik_1(A-B) = k_2(C-D). \tag{2.20}$$

For the second boundary, i.e. $x = L$, we have

$$Ce^{k_2 L} + De^{-k_2 L} = Ee^{ik_1 L}, \tag{2.21}$$

from

$$\psi_2(L) = \psi_3(L). \tag{2.22}$$

The derivatives

$$\dot{\psi}_2(L) = \dot{\psi}_3(L), \tag{2.23}$$

inturn give

$$k_2(Ce^{k_2 L} - De^{-k_2 L}) = ik_1 Ee^{ik_1 L}. \tag{2.24}$$

From (2.21) and (2.24) we have the two coefficients

$$C = \frac{E}{2}\left(1 + i\frac{k_1}{k_2}\right)e^{(ik_1 - k_2)L}, \tag{2.25}$$

$$D = \frac{E}{2}\left(1 - i\frac{k_1}{k_2}\right)e^{(ik_1 + k_2)L}. \tag{2.26}$$

Plugging these two coefficients into (2.18) and (2.20) and solving the resulting two equations for $\frac{B}{A}$ and $\frac{E}{A}$ we get

$$\frac{E}{A} = 2e^{-ik_1 L}\left[2\cosh(k_2 L) + i\left(\frac{k_2^2 - k_1^2}{k_1 k_2}\right)\sinh(k_2 L)\right]^{-1} \tag{2.27}$$

and

$$\frac{B}{A} = -i\frac{k_1^2 + k_2^2}{k_1 k_2}\sinh(k_2 L)\left[2\cosh(k_2 L) + i\left(\frac{k_2^2 - k_1^2}{k_1 k_2}\right)\sinh(k_2 L)\right]^{-1}. \tag{2.28}$$

Absolute square of (2.27) and (2.28) give us the transmission and reflection coefficients respectively. They read

$$T = 4\left[4\cosh^2(k_2 L) + \left(\frac{k_2^2 - k_1^2}{k_1 k_2}\right)^2 \sinh^2(k_2 L)\right]^{-1}, \tag{2.29}$$

$$R = \left(\frac{k_1^2 + k_2^2}{k_1 k_2}\right)^2 \sinh^2(k_2 L)\left[4\cosh^2(k_2 L) + \left(\frac{k_2^2 - k_1^2}{k_1 k_2}\right)^2 \sinh^2(k_2 L)\right]^{-1}. \tag{2.30}$$

2.4. Tunneling in Polymer Representation

In this section, we will investigate the tunneling problem using the polymer representation. The shape of the potential barrier is given below in Figure 2.2. As it is depicted in the figure, we study the problem by dividing the potential into three regions. In each region we solve the relevant eigenvalue equation and find the wave function in that region. In the end, we apply the boundary conditions and calculate the transmission and reflection coefficients. A remark is in order about the potential profile here: the barrier width is assumed to be $L = N\mu_0$, where μ_0 is the fundamental length scale in polymer representation and N is an integer.

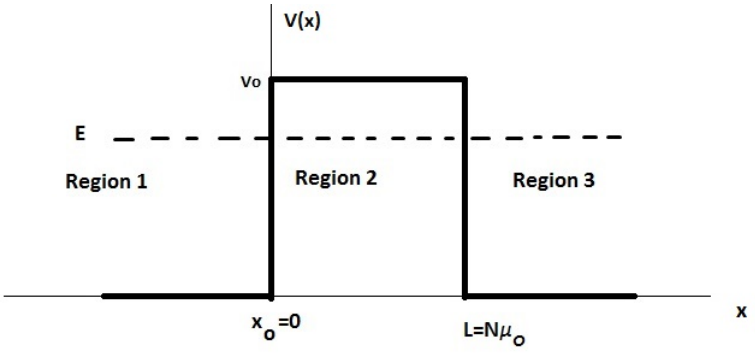

Figure 2.2. Shape of the potential barrier used to examine tunneling in polymer framework. Note that the barrier width is divided into discrete pieces of length μ_0, which is called the fundamental length scale.

2.4.1. Region 1

In this region, the Hamiltonian takes the form of a free particle, namely :

$$\hat{H}_1 = \frac{\hbar^2}{2m\mu_0^2}\left[2 - \hat{V}(\mu_0) - \hat{V}(-\mu_0)\right]. \tag{2.31}$$

Using the fact that $x_j = x_0 + j\mu_0$ and defining the state vectors in the polymer framework as $|\psi\rangle = \sum_{j\in\mathbb{Z}} \psi(x_j)|x_j\rangle$ the eigenvalue equation $\hat{H}_{\mu_0}|\psi\rangle = E|\psi\rangle$ takes the form:

$$\frac{\hbar^2}{2m\mu_0^2}\Big[2\psi(x_j) - \psi(x_j - \mu_0) - \psi(x_j + \mu_0)\Big] = E\psi(x_j). \tag{2.32}$$

After making the redefinition $x_j \equiv j+1$ we obtain

$$\frac{\hbar^2}{2m\mu_0^2}\Big[2\psi(j+1)-\psi(j)-\psi(j+2)\Big]=E\psi(j+1). \tag{2.33}$$

collecting the terms, equation (2.33) becomes:

$$\psi(j+2)-\left(2-\frac{2mE\mu_0^2}{\hbar^2}\right)\psi(j+1)+\psi(j)=0\,. \tag{2.34}$$

The solution of this second order difference equation is proposed to be

$$\psi(j)=a_+r_+^j+a_-r_-^j \tag{2.35}$$

where $a_\pm$ are constant coefficients and the roots of the characteristic equation

$$r^2-\left(2-\frac{2mE\mu_0^2}{\hbar^2}\right)r+1=0, \tag{2.36}$$

$r_\pm$, are given by:

$$r_\pm=\left(1-\frac{mE\mu_0^2}{\hbar^2}\right)\pm\frac{1}{2}\sqrt{\frac{8mE\mu_0^2}{\hbar^2}\left(\frac{mE\mu_0^2}{2\hbar^2}-1\right)}\,. \tag{2.37}$$

Equation (2.37) can be written in the following simpler form; $r_\pm=\varepsilon\pm\sqrt{\varepsilon^2-1}$ where $\varepsilon\equiv\left(1-\frac{mE\mu_0^2}{\hbar^2}\right)$. In order to obtain physical solutions in *Region 1* the roots of the characteristic equation should be complex numbers; that is $\varepsilon^2<1$. This leads to the idea that the minimum length scale μ_0 imposes a cut-off on the energy; namely we should have $E<\frac{2\hbar^2}{m\mu_0^2}$. Using this fact, the wave function becomes

$$\psi(j)=a_+\left(\varepsilon+i\sqrt{1-\varepsilon^2}\right)^j+a_-\left(\varepsilon-i\sqrt{1-\varepsilon^2}\right)^j\,. \tag{2.38}$$

We can write this equation in polar coordinates by defining

$$\varepsilon\equiv\cos\theta\quad and$$
$$\sqrt{1-\varepsilon^2}=\sin\theta\,.$$

The result becomes

$$\psi_1(j)=a_1(\cos\theta+i\sin\theta)^j+a_2(\cos\theta-i\sin\theta)^j \tag{2.39}$$

which is equal to

$$\psi_1(j)=a_1e^{ij\theta}+a_2e^{-ij\theta} \tag{2.40}$$

where $\theta = \arccos(\varepsilon)$. Plugging in the values of θ and ε, equation (2.40) becomes

$$\psi_1(j) = a_1 e^{ij \arccos(1-\frac{m\mu_0^2}{\hbar^2}E)} + a_2 e^{-ij \arccos(1-\frac{m\mu_0^2}{\hbar^2}E)} \ . \tag{2.41}$$

2.4.2. Region 2:

Inside the barrier region, the Hamiltonian takes the form:

$$\hat{H}_2 = \frac{\hbar^2}{2m\mu_0^2}\left[2 - \hat{V}(\mu_0) - \hat{V}(-\mu_0)\right] + \hat{V}_0 \tag{2.42}$$

The eigenvalue equation $\hat{H}_{\mu_0}|\psi\rangle = E|\psi\rangle$ becomes in this region

$$\frac{\hbar^2}{2m\mu_0^2}\left[2\psi(x_j) - \hat{V}(\mu_0)\psi(x_j) - \hat{V}(-\mu_0)\psi(x_j)\right] + V_0\psi(x_j) = E\psi(x_j). \tag{2.43}$$

Making the same redefinition as above, i.e. $x_j \equiv j+1$, this takes the form

$$2\psi(j+1) - \psi(j) - \psi(j+2) - \frac{2m\mu_0^2}{\hbar^2}\left(E - V_0\right)\psi(j+1) = 0 \ . \tag{2.44}$$

Rearranging the terms we get

$$\psi(j+2) - \left(2 - \frac{2m(E-V_0)\mu_0^2}{\hbar^2}\right)\psi(j+1) + \psi(j) = 0. \tag{2.45}$$

The characteristic equation corresponding to this difference equation is

$$r^2 - \left(2 - \frac{2m(E-V_0)\mu_0^2}{\hbar^2}\right)r + 1 = 0. \tag{2.46}$$

The roots of this characteristic equation are

$$r_\pm = \lambda \pm \sqrt{\lambda^2 - 1} \tag{2.47}$$

where

$$\lambda \equiv \left(1 - \frac{m(E-V_0)\mu_0^2}{\hbar^2}\right). \tag{2.48}$$

For real and distinct roots $\lambda^2 > 1$. In that case, the proposed solution of the difference equation takes the form

$$\psi_2(j) = b_1(\lambda + \sqrt{\lambda^2-1})^j + b_2(\lambda - \sqrt{\lambda^2-1})^j. \tag{2.49}$$

Which, by making the definition $\lambda \equiv \cosh\phi$, becomes

$$\psi_2(j) = b_1 e^{j\phi} + b_2 e^{-j\phi} \tag{2.50}$$

where $\phi = \operatorname{arccosh}\left(1 - \frac{m(E-V_0)\mu_0^2}{\hbar^2}\right)$. Hence, the wave function in this region is

$$\psi_2(j) = b_1 e^{j\operatorname{arccosh}\left(1-\frac{m(E-V_0)\mu_0^2}{\hbar^2}\right)} + b_2 e^{-j\operatorname{arccosh}\left(1-\frac{m(E-V_0)\mu_0^2}{\hbar^2}\right)}. \tag{2.51}$$

2.4.3. Region 3:

Region 3 has the same Hamiltonian as Region 1, namely equation (2.31). The characteristic equation has the roots (2.37) and they are written compactly as $r_\pm = \varepsilon \pm \sqrt{\varepsilon^2 - 1}$. For complex roots, i.e. a physical wave function, we should have $\epsilon^2 < 1$. The wave function, as in the first region , is

$$\psi_3(j) = c_1 e^{ij\arccos\varepsilon} + c_2 e^{-ij\arccos\varepsilon} \tag{2.52}$$

but since on the right side of the barrier we should have only a right propagating wave, the coefficient c_2 of the second term must be zero. Hence, the wave function reduces to

$$\psi_3(j) = c_1 e^{ij\arccos\left(1-\frac{m\mu_0^2}{\hbar^2}E\right)}. \tag{2.53}$$

2.4.4. Transmission and Reflection Coefficients

Conservation of probability current dictates that we equate the wave-functions and their derivatives at the boundaries. At the left-end of the barrier,

$$\psi_1(0) = \psi_2(0) \tag{2.54}$$

gives us

$$a_1 + a_2 = b_1 + b_2. \tag{2.55}$$

At the right-end

$$\psi_2(N) = \psi_3(N) \tag{2.56}$$

returns

$$b_1 e^{N\operatorname{arccosh}(\lambda)} + b_2 e^{-N\operatorname{arccosh}(\lambda)} = c_1 e^{iN\arccos(\varepsilon)}. \tag{2.57}$$

Derivatives of the wave function are calculated using the definition of derivative as a limit. The derivative of the wave function of the first region at $x = 0$ is defined as

$$\left.\frac{d\psi_1}{dx}\right|_{x=0} = \frac{\psi_1(j=0) - \psi_1(j=-1)}{\mu_0} \ . \tag{2.58}$$

Setting $j = 0$ and $j = -1$ in (2.41), we obtain the following respectively

$$\psi_1(j=0) = a_1 + a_2 \tag{2.59}$$

and

$$\psi_1(j=-1) = a_1 e^{-i\arccos(\varepsilon)} + a_2 e^{i\arccos(\varepsilon)} \ . \tag{2.60}$$

Inserting these in (2.58), results

$$\left.\frac{d\psi_1}{dx}\right|_{x=0} = \frac{a_1\left(1 - e^{-i\arccos(\varepsilon)}\right) + a_2\left(1 - e^{i\arccos(\varepsilon)}\right)}{\mu_0} \ . \tag{2.61}$$

Following the same procedure for the wave function of the second region, we write the derivative of the wave function of the second region at $x = 0$ as

$$\left.\frac{d\psi_2}{dx}\right|_{x=0} = \frac{\psi_2(j=1) - \psi_2(j=0)}{\mu_0} \ . \tag{2.62}$$

Setting $j = 1$ and $j = 0$ in (2.51), we obtain the following two equations respectively

$$\psi_2(j=1) = b_1 e^{\operatorname{arccosh}(\lambda)} + b_2 e^{-\operatorname{arccosh}(\lambda)} \tag{2.63}$$

and

$$\psi_2(j=0) = b_1 + b_2 \ . \tag{2.64}$$

Inserting these in (2.62), results

$$\left.\frac{d\psi_2}{dx}\right|_{x=0} = \frac{b_1\left(e^{\operatorname{arccosh}(\lambda)} - 1\right) + b_2\left(e^{-\operatorname{arccosh}(\lambda)} - 1\right)}{\mu_0} \ . \tag{2.65}$$

For the left end of the barrier we have

$$\left.\frac{d\psi_2}{dx}\right|_{x=L} = \frac{\psi_2(j=N) - \psi_2(j=N-1)}{\mu_0} \ . \tag{2.66}$$

Setting $j = N$ and $j = N-1$ in (2.51), we obtain the following two equations respectively

$$\psi_2(j=N) = b_1 e^{N\text{arccosh}(\lambda)} + b_2 e^{-N\text{arccosh}(\lambda)} \tag{2.67}$$

and

$$\psi_2(j=N-1) = b_1 e^{(N-1)\text{arccosh}(\lambda)} + b_2 e^{-(N-1)\text{arccosh}(\lambda)} \ . \tag{2.68}$$

Inserting these in (2.66), results

$$\left.\frac{d\psi_2}{dx}\right|_{x=L} = \frac{b_1\left(e^{\text{arccosh}(\lambda)} - 1\right)e^{(N-1)\text{arccosh}(\lambda)} + b_2\left(e^{-\text{arccosh}(\lambda)} - 1\right)e^{-(N-1)\text{arccosh}(\lambda)}}{\mu_0} \ . \tag{2.69}$$

The derivative of the wave function of the third region reads

$$\left.\frac{d\psi_3}{dx}\right|_{x=L} = \frac{\psi_3(j=N+1) - \psi_3(j=N)}{\mu_0} \ . \tag{2.70}$$

We have

$$\psi_3(j=N+1) = c_1 e^{i(N+1)\arccos\varepsilon} \tag{2.71}$$

and

$$\psi_3(j=N) = c_1 e^{iN\arccos\varepsilon} \tag{2.72}$$

for the wave functions at $j = N+1$ and $j = N$. When we plug these two equations into (2.70) we obtain

$$\left.\frac{d\psi_3}{dx}\right|_{x=L} = \frac{c_1 e^{iN\arccos\varepsilon}\left(e^{i\arccos\varepsilon} - 1\right)}{\mu_0} \ . \tag{2.73}$$

Equating the derivatives of the wave function at the left and the right-ends, result in the following equations respectively:

$$\left.\frac{d\psi_1}{dx}\right|_{x=0} = \left.\frac{d\psi_2}{dx}\right|_{x=0} \tag{2.74}$$

leads to

$$\begin{aligned} a_1\left(1 - e^{-i\arccos(\varepsilon)}\right) + a_2\left(1 - e^{i\arccos(\varepsilon)}\right) = \ & b_1 \left(e^{\text{arccosh}(\lambda)} - 1\right) + \\ & b_2 \left(e^{-\text{arccosh}(\lambda)} - 1\right) \ . \end{aligned} \tag{2.75}$$

$$\left.\frac{d\psi_2}{dx}\right|_{x=L} = \left.\frac{d\psi_3}{dx}\right|_{x=L} \tag{2.76}$$

gives

$$\begin{aligned} b_1 \quad & \left(e^{\text{arccosh}(\lambda)} - 1\right) e^{(N-1)\text{arccosh}(\lambda)} + b_2 \left(e^{-\text{arccosh}(\lambda)} - 1\right) e^{-(N-1)\text{arccosh}(\lambda)} = \\ c_1 \quad & \left(e^{i\arccos(\varepsilon)} - 1\right) e^{iN\arccos(\varepsilon)}. \end{aligned} \tag{2.77}$$

Solving equations (2.55), (2.57), (2.75) and (2.77) simultaneously we find the analytical expressions for the coefficients a_1, a_2, b_1 and b_2 in terms of the undetermined coefficient c_1:

$$\begin{aligned} a_1 \;=\; & \frac{c_1 e^{iN\arccos(\varepsilon)}}{\left(e^{2\text{arccosh}(\lambda)} - 1\right)\left(e^{i\arccos(\varepsilon)} - e^{-i\arccos(\varepsilon)}\right)} \Big(e^{(3-N)\text{arccosh}(\lambda)} \\ & - 4e^{(2-N)\text{arccosh}(\lambda)} + 2e^{i\arccos(\varepsilon)+(2-N)\text{arccosh}(\lambda)} - 4e^{i\arccos(\varepsilon)+(1-N)\text{arccosh}(\lambda)} \\ & + e^{2i\arccos(\varepsilon)+(1-N)\text{arccosh}(\lambda)} + 4e^{(1-N)\text{arccosh}(\lambda)} + 4e^{i\arccos(\varepsilon)+(N+1)\text{arccosh}(\lambda)} \\ & - 2e^{i\arccos(\varepsilon)+N\text{arccosh}(\lambda)} - e^{(N-1)\text{arccosh}(\lambda)} + 4e^{N\text{arccosh}(\lambda)} - 4e^{(N+1)\text{arccosh}(\lambda)} \\ & - e^{2i\arccos(\varepsilon)+(N+1)\text{arccosh}(\lambda)} \Big) \end{aligned} \tag{2.78}$$

$$\begin{aligned} a_2 \;=\; & \frac{c_1 e^{iN\arccos(\varepsilon)}}{\left(e^{2\text{arccosh}(\lambda)} - 1\right)\left(e^{i\arccos(\varepsilon)} - e^{-i\arccos(\varepsilon)}\right)} \Big(- e^{i\arccos(\varepsilon)+(2-N)\text{arccosh}(\lambda)} \\ & + 2e^{i\arccos(\varepsilon)+(1-N)\text{arccosh}(\lambda)} - 2e^{i\arccos(\varepsilon)+(N+1)\text{arccosh}(\lambda)} - e^{(3-N)\text{arccosh}(\lambda)} \\ & - e^{-i\arccos(\varepsilon)+(2-N)\text{arccosh}(\lambda)} + 2e^{-i\arccos(\varepsilon)+(1-N)\text{arccosh}(\lambda)} - 5e^{(1-N)\text{arccosh}(\lambda)} \\ & - 2e^{-i\arccos(\varepsilon)+(N+1)\text{arccosh}(\lambda)} + 5e^{(N+1)\text{arccosh}(\lambda)} + e^{-i\arccos(\varepsilon)+N\text{arccosh}(\lambda)} \\ & + 4e^{(2-N)\text{arccosh}(\lambda)} - 4e^{N\text{arccosh}(\lambda)} + e^{(N-1)\text{arccosh}(\lambda)} + e^{i\arccos(\varepsilon)+N\text{arccosh}(\lambda)} \Big) \end{aligned} \tag{2.79}$$

$$b_1 = \left(c_1 e^{iN\arccos(\varepsilon)}\right) \frac{\left(e^{(2-N)\text{arccosh}(\lambda)} - 2e^{(1-N)\text{arccosh}(\lambda)} + e^{i\arccos(\varepsilon)+(1-N)\text{arccosh}(\lambda)}\right)}{\left(e^{2\text{arccosh}(\lambda)} - 1\right)} \tag{2.80}$$

$$b_2 = \left(c_1 e^{iN\arccos(\varepsilon)}\right) \frac{\left(2e^{(N+1)\text{arccosh}(\lambda)} - e^{i\arccos(\varepsilon)+(N+1)\text{arccosh}(\lambda)} - e^{N\text{arccosh}(\lambda)}\right)}{\left(e^{2\text{arccosh}(\lambda)} - 1\right)} \tag{2.81}$$

The transmission and reflection coefficients are defined respectively as $T = \frac{|c_1|^2}{|a_1|^2}$ and $R = \frac{|a_2|^2}{|a_1|^2}$ .When we plug the values of a_1 and a_2 in the transmission and reflection coefficients and sum them it is easily obtained that $T + R = 1$, which is the requirement of probability conservation. [1]

[1] Calculation of the explicit expressions for T and R are given in the Appendix B.1.

CHAPTER 3

TUNNELING-TIME AND QUANTUM ZENO EFFECT

3.1. Tunneling-time in Polymer Representation

Time and position are not treated on an equal footing in quantum theory. Position is represented by an operator whereas time is left as just a parameter. Here, in our work, we end this dichotomy between time and position by elevating time to the status of being represented by an operator. First of all, we define our time-operator and then use it to calculate the time it takes for a quantum particle to tunnel through the potential barrier given in Figure 2.2.

We define our differential time-operator as :

$$d\hat{T} = \left|\frac{m d\hat{x}}{\hat{p}}\right|. \tag{3.1}$$

The reason why we define our differential time operator through an absolute value sign is that we have to make sure that the differential length, $d\hat{x}$, and momentum, $\hat{p}$, of the particle point in the same direction so that when we integrate out the differential time operator we get the tunneling time that corresponds to transmission. When we use the regularized momentum operator, $\hat{p} = \frac{\hbar}{i2\mu_0}\left(\hat{V}(\mu_0) - \hat{V}(-\mu_0)\right)$, in (3.1) we get:

$$d\hat{T} = \left|\left(\frac{i2m\mu_0}{\hbar}\right)\frac{d\hat{x}}{\hat{V}(\mu_0) - \hat{V}(-\mu_0)}\right|. \tag{3.2}$$

Tunneling-time is the expectation value of the integral of differential time-operator from the left-end of the barrier, $x = 0$, to the right-end, $x = L$. Hence, we can write tunneling time as:

$$T = \langle\psi|\left|\left(\int_0^L \left(\frac{i2m\mu_0}{\hbar}\right)\frac{d\hat{x}}{\hat{V}(\mu_0) - \hat{V}(-\mu_0)}\right)\right||\psi\rangle \tag{3.3}$$

In our analysis we are going to work in the position basis since we have a better knowledge of the position of the particle during the tunneling process. But in order to do that, we have to regularize the momentum operator somehow and bring the expression in the denominator of the time operator, i.e. $\hat{V}(\mu_0) - \hat{V}(-\mu_0)$, up into the nominator because position eigenkets

are not eigenkets of the operator $\hat{V}(\mu_0)$. For this purpose, we will use the regularization

$$\frac{1}{\hat{V}(\mu_0)-\hat{V}(-\mu_0)} = \int_0^\infty e^{-a\left(\hat{V}(\mu_0)-\hat{V}(-\mu_0)\right)} da \tag{3.4}$$

and then employ the series expansion formula

$$e^{-a\left(\hat{V}(\mu_0)-\hat{V}(-\mu_0)\right)} = \sum_{n=0}^{\infty} \frac{\left(\hat{V}(\mu_0)-\hat{V}(-\mu_0)\right)^n (-a)^n}{n!} \tag{3.5}$$

for the exponential. After inserting (3.5) into (3.4), we plug (3.4) into (3.3) and get

$$T = \langle\psi| \left| \left(\int_0^L \left(\frac{i2m\mu_0}{\hbar}\right) d\hat{x} \int_0^\infty \sum_{n=0}^{\infty} \frac{\left(\hat{V}(\mu_0)-\hat{V}(-\mu_0)\right)^n (-a)^n}{n!}\ da \right) \right| |\psi\rangle \ . \tag{3.6}$$

Now we insert the identity operators between the wave functions and the time operator. The result becomes:

$$T = \left| \left(\frac{i2mN\mu_0^2}{\hbar}\right) \sum_{j,k} \psi_j^* \langle x_j| \left(\int_0^\infty \sum_{n=0}^{\infty} \frac{\left(\hat{V}(\mu_0)-\hat{V}(-\mu_0)\right)^n (-a)^n}{n!} da \right) |x_k\rangle \psi_k \right| \tag{3.7}$$

where we denote $\psi(x_j)$ as ψ_j for the sake of brevity. To get a feel for the form that will be taken by (3.7), we expand the first couple of terms of the summation inside the integral

$$\begin{aligned} \langle x_j| \left(\int_0^\infty \sum_{n=0}^{\infty} \frac{\left(\hat{V}(\mu_0)-\hat{V}(-\mu_0)\right)^n (-a)^n}{n!}\ da \right) |x_k\rangle = \int_0^\infty da \Bigg\{ \langle x_j|1|x_k\rangle - \\ \frac{a\langle x_j| \left[\hat{V}(\mu_0)-\hat{V}(-\mu_0)\right] |x_k\rangle}{1!} + \frac{a^2\langle x_j| \left[\hat{V}(\mu_0)-\hat{V}(-\mu_0)\right]^2 |x_k\rangle}{2!} - \\ \frac{a^3\langle x_j| \left[\hat{V}(\mu_0)-\hat{V}(-\mu_0)\right]^3 |x_k\rangle}{3!} + \dots \Bigg\} . \end{aligned} \tag{3.8}$$

In order to further evaluate this expression, we need to expand $[\hat{V}(\mu_0)-\hat{V}(-\mu_0)]^2$ and $[\hat{V}(\mu_0)-\hat{V}(-\mu_0)]^3$. They are calculated using the additivity property of the one parameter unitary groups and read as follows

$$[\hat{V}(\mu_0)-\hat{V}(-\mu_0)]^2 = \hat{V}(2\mu_0)+\hat{V}(-2\mu_0)-2 \tag{3.9}$$

and

$$[\hat{V}(\mu_0)-\hat{V}(-\mu_0)]^3 = \hat{V}(3\mu_0)-3\hat{V}(\mu_0)+3\hat{V}(-\mu_0)-\hat{V}(-3\mu_0). \tag{3.10}$$

Inserting these two equations into (3.8) we obtain

$$\langle x_j| \left(\int_0^\infty \sum_{n=0}^{\infty} \frac{\left(\hat{V}(\mu_0) - \hat{V}(-\mu_0)\right)^n (-a)^n}{n!} \; da \right) |x_k\rangle = \int_0^\infty da \Bigg\{ \langle x_j|1|x_k\rangle - \\ \frac{a\langle x_j| \left[\hat{V}(\mu_0) - \hat{V}(-\mu_0)\right] |x_k\rangle}{1!} + \frac{a^2\langle x_j| \left[\hat{V}(2\mu_0) + \hat{V}(-2\mu_0) - 2\right] |x_k\rangle}{2!} - \\ \frac{a^3\langle x_j| \left[\hat{V}(3\mu_0) - 3\hat{V}(\mu_0) + 3\hat{V}(-\mu_0) - \hat{V}(-3\mu_0)\right] |x_k\rangle}{3!} + \dots \Bigg\} . \tag{3.11}$$

Next, we distribute $\langle x_j|$ and $|x_k\rangle$ into the square brackets in (3.11)

$$\langle x_j| \left(\int_0^\infty \sum_{n=0}^{\infty} \frac{\left(\hat{V}(\mu_0) - \hat{V}(-\mu_0)\right)^n (-a)^n}{n!} \; da \right) |x_k\rangle = \int_0^\infty da \Bigg\{ \langle x_j|x_k\rangle - \\ \frac{a}{1!}\Big[\langle x_j|\hat{V}(\mu_0)|x_k\rangle - \langle x_j|\hat{V}(-\mu_0)|x_k\rangle\Big] + \frac{a^2}{2!}\Big[\langle x_j|\hat{V}(2\mu_0)|x_k\rangle + \langle x_j|\hat{V}(-2\mu_0)|x_k\rangle - \\ 2\langle x_j|x_k\rangle\Big] - \frac{a^3}{3!}\Big[\langle x_j|\hat{V}(3\mu_0)|x_k\rangle - 3\langle x_j|\hat{V}(\mu_0)|x_k\rangle + 3\langle x_j|\hat{V}(-\mu_0)|x_k\rangle - \\ \langle x_j|\hat{V}(-3\mu_0)|x_k\rangle\Big] + \dots \Bigg\} . \tag{3.12}$$

Making use of (1.19), (3.12) takes the form

$$\langle x_j| \left(\int_0^\infty \sum_{n=0}^{\infty} \frac{\left(\hat{V}(\mu_0) - \hat{V}(-\mu_0)\right)^n (-a)^n}{n!} \; da \right) |x_k\rangle = \int_0^\infty da \Bigg\{ \langle x_j|x_k\rangle - \\ \frac{a}{1!}\Big[\langle x_j|x_{k-1}\rangle - \langle x_j|x_{k+1}\rangle\Big] + \frac{a^2}{2!}\Big[\langle x_j|x_{k-2}\rangle + \langle x_j|x_{k+2}\rangle - 2\langle x_j|x_k\rangle\Big] - \\ \frac{a^3}{3!}\Big[\langle x_j|x_{k-3}\rangle - 3\langle x_j|x_{k-1}\rangle + 3\langle x_j|x_{k+1}\rangle - \langle x_j|x_{k+3}\rangle\Big] + \dots \Bigg\} . \tag{3.13}$$

In terms of Kronecker Deltas (3.13) can be written as

$$\langle x_j| \left(\int_0^\infty \sum_{n=0}^{\infty} \frac{\left(\hat{V}(\mu_0) - \hat{V}(-\mu_0)\right)^n (-a)^n}{n!} \; da \right) |x_k\rangle = \int_0^\infty da \Bigg\{ \delta_{j,k} - \\ \frac{a}{1!}\Big[\delta_{j,k-1} - \delta_{j,k+1}\Big] + \frac{a^2}{2!}\Big[\delta_{j,k-2} + \delta_{j,k+2} - 2\delta_{j,k}\Big] - \\ \frac{a^3}{3!}\Big[\delta_{j,k-3} - 3\delta_{j,k-1} + 3\delta_{j,k+1} - \delta_{j,k+3}\Big] + \dots \Bigg\} . \tag{3.14}$$

Next, we insert (3.14) into (3.7)

$$T = \left| \left(\frac{i2mN\mu_0^2}{\hbar} \right) \sum_{j,k} \psi_j^* \left(\int_0^\infty da \left\{ \delta_{j,k} - \frac{a}{1!}\Big[\delta_{j,k-1} - \delta_{j,k+1}\Big] + \right.\right.$$
$$\frac{a^2}{2!}\Big[\delta_{j,k-2} + \delta_{j,k+2} - 2\delta_{j,k}\Big] - \frac{a^3}{3!}\Big[\delta_{j,k-3} - 3\delta_{j,k-1} + 3\delta_{j,k+1} - \delta_{j,k+3}\Big] \qquad (3.15)$$
$$\left.\left. + \dots \right\} \right) \psi_k \right| .$$

Throwing ψ_j^* and ψ_k in the curly brackets we obtain

$$T = \left| \left(\frac{i2mN\mu_0^2}{\hbar} \right) \int_0^\infty da \sum_{j,k} \left\{ \psi_j^* \delta_{j,k} \psi_k - \frac{a}{1!}\Big[\psi_j^* \delta_{j,k-1}\psi_k - \psi_j^* \delta_{j,k+1}\psi_k\Big] + \right.$$
$$\frac{a^2}{2!}\Big[\psi_j^* \delta_{j,k-2}\psi_k + \psi_j^* \delta_{j,k+2}\psi_k - 2\psi_j^* \delta_{j,k}\psi_k\Big] - \frac{a^3}{3!}\Big[\psi_j^* \delta_{j,k-3}\psi_k - 3\psi_j^* \delta_{j,k-1}\psi_k + \qquad (3.16)$$
$$\left. 3\psi_j^* \delta_{j,k+1}\psi_k - \psi_j^* \delta_{j,k+3}\psi_k\Big] + \dots \right\} \right| .$$

Affecting the Kronecker Deltas on the wave functions we get

$$T = \left| \left(\frac{i2mN\mu_0^2}{\hbar} \right) \int_0^\infty da \sum_{k} \left\{ |\psi_k|^2 - \frac{a}{1!}\Big[\psi_{k-1}^* \psi_k - \psi_{k+1}^* \psi_k\Big] + \right.$$
$$\frac{a^2}{2!}\Big[\psi_{k-2}^* \psi_k + \psi_{k+2}^* \psi_k - 2|\psi_k|^2\Big] - \frac{a^3}{3!}\Big[\psi_{k-3}^* \psi_k - 3\psi_{k-1}^* \psi_k + \qquad (3.17)$$
$$\left. 3\psi_{k+1}^* \psi_k - \psi_{k+3}^* \psi_k\Big] + \dots \right\} \right| .$$

At this point in the calculation we have to evaluate terms such as $\psi_{k-1}^* \psi_k$ in (3.17). For this purpose we will use the wave function pertaining to the second region of the tunneling potential, i.e. ψ_2 in equation (2.51). From that equation we can write ψ_k and its complex conjugate as follows

$$\psi_k = b_1 e^{k \operatorname{arccosh} \lambda} + b_2 e^{-k \operatorname{arccosh} \lambda} \qquad (3.18)$$

$$\psi_k^* = b_1^* e^{k \operatorname{arccosh} \lambda} + b_2^* e^{-k \operatorname{arccosh} \lambda} . \qquad (3.19)$$

Multiplying (3.19) with (3.18) we obtain $|\psi_k|^2$

$$|\psi_k|^2 = |b_1|^2 e^{2k \operatorname{arccosh} \lambda} + b_1^* b_2 + b_2^* b_1 + |b_2|^2 e^{-2k \operatorname{arccosh} \lambda} . \qquad (3.20)$$

Substituting $k-1$ for k in (3.19) we have

$$\psi_{k-1}^* = b_1^* e^{(k-1) \operatorname{arccosh} \lambda} + b_2^* e^{-(k-1) \operatorname{arccosh} \lambda} . \qquad (3.21)$$

Multiplication of (3.21) with (3.18) gives us

$$\psi_{k-1}^{*}\psi_k = |b_1|^2 e^{(2k-1)\,\mathrm{arccosh}\,\lambda} + b_1^{*}b_2 e^{-\,\mathrm{arccosh}\,\lambda} + b_2^{*}b_1 e^{\,\mathrm{arccosh}\,\lambda} + |b_2|^2 e^{-(2k-1)\,\mathrm{arccosh}\,\lambda}\,. \quad (3.22)$$

Similar calculations lead to

$$\psi_{k+1}^{*}\psi_k = |b_1|^2 e^{(2k+1)\,\mathrm{arccosh}\,\lambda} + b_1^{*}b_2 e^{\,\mathrm{arccosh}\,\lambda} + b_2^{*}b_1 e^{-\,\mathrm{arccosh}\,\lambda} + |b_2|^2 e^{-(2k+1)\,\mathrm{arccosh}\,\lambda}\,, \quad (3.23)$$

$$\psi_{k-2}^{*}\psi_k = |b_1|^2 e^{(2k-2)\,\mathrm{arccosh}\,\lambda} + b_1^{*}b_2 e^{-2\,\mathrm{arccosh}\,\lambda} + b_2^{*}b_1 e^{2\,\mathrm{arccosh}\,\lambda} + |b_2|^2 e^{-(2k-2)\,\mathrm{arccosh}\,\lambda}\,, \quad (3.24)$$

$$\psi_{k+2}^{*}\psi_k = |b_1|^2 e^{(2k+2)\,\mathrm{arccosh}\,\lambda} + b_1^{*}b_2 e^{2\,\mathrm{arccosh}\,\lambda} + b_2^{*}b_1 e^{-2\,\mathrm{arccosh}\,\lambda} + |b_2|^2 e^{-(2k+2)\,\mathrm{arccosh}\,\lambda}\,, \quad (3.25)$$

$$\psi_{k-3}^{*}\psi_k = |b_1|^2 e^{(2k-3)\,\mathrm{arccosh}\,\lambda} + b_1^{*}b_2 e^{-3\,\mathrm{arccosh}\,\lambda} + b_2^{*}b_1 e^{3\,\mathrm{arccosh}\,\lambda} + |b_2|^2 e^{-(2k-3)\,\mathrm{arccosh}\,\lambda} \quad (3.26)$$

and

$$\psi_{k+3}^{*}\psi_k = |b_1|^2 e^{(2k+3)\,\mathrm{arccosh}\,\lambda} + b_1^{*}b_2 e^{3\,\mathrm{arccosh}\,\lambda} + b_2^{*}b_1 e^{-3\,\mathrm{arccosh}\,\lambda} + |b_2|^2 e^{-(2k+3)\,\mathrm{arccosh}\,\lambda}\,. \quad (3.27)$$

Now it is time to make use of equations (3.22) through (3.27) and (3.20) to obtain the terms within the square brackets in (3.17), they respectively read

$$\left[\psi_{k-1}^{*}\psi_k - \psi_{k+1}^{*}\psi_k\right] = \left(e^{-\,\mathrm{arccosh}\,\lambda} - e^{\,\mathrm{arccosh}\,\lambda}\right)\Big\{|b_1|^2 e^{2k\,\mathrm{arccosh}\,\lambda} + b_1^{*}b_2 - b_2^{*}b_1 - |b_2|^2 e^{-2k\,\mathrm{arccosh}\,\lambda}\Big\}\,, \quad (3.28)$$

$$\left[\psi_{k-2}^{*}\psi_k + \psi_{k+2}^{*}\psi_k - 2|\psi_k|^2\right] = \left(e^{\,\mathrm{arccosh}\,\lambda} - e^{-\,\mathrm{arccosh}\,\lambda}\right)^2\Big\{|b_1|^2 e^{2k\,\mathrm{arccosh}\,\lambda} + b_1^{*}b_2 + b_2^{*}b_1 + |b_2|^2 e^{-2k\,\mathrm{arccosh}\,\lambda}\Big\} \quad (3.29)$$

and

$$\left[\psi_{k-3}^{*}\psi_k - 3\psi_{k-1}^{*}\psi_k + 3\psi_{k+1}^{*}\psi_k - \psi_{k+3}^{*}\psi_k\right] = \left(e^{-\mathrm{arccosh}\lambda} - e^{\mathrm{arccosh}\lambda}\right)^3\Big\{|b_1|^2 e^{2k\mathrm{arccosh}\lambda} + b_1^{*}b_2 - b_2^{*}b_1 - |b_2|^2 e^{-2k\,\mathrm{arccosh}\,\lambda}\Big\}\,. \quad (3.30)$$

Inserting (3.20), (3.28), (3.29) and (3.30) in (3.17) we obtain the expression below.

$$
\begin{aligned}
T &= \left| \left(\frac{i2mN\mu_0^2}{\hbar} \right) \sum_k \int_0^\infty da \Big[\Big(|b_1|^2 e^{2k\mathrm{arccosh}(\lambda)} + b_1^* b_2 + b_2^* b_1 + \right. \qquad (3.31) \\
&+ |b_2|^2 e^{-2k\mathrm{arccosh}(\lambda)} \Big) - \frac{a}{1!} \left(e^{-\mathrm{arccosh}(\lambda)} - e^{\mathrm{arccosh}(\lambda)} \right) \Big(|b_1|^2 e^{2k\mathrm{arccosh}(\lambda)} + b_1^* b_2 - \\
&- b_2^* b_1 - |b_2|^2 e^{-2k\mathrm{arccosh}(\lambda)} \Big) + \frac{a^2}{2!} \left(e^{\mathrm{arccosh}(\lambda)} - e^{-\mathrm{arccosh}(\lambda)} \right)^2 \Big(|b_1|^2 e^{2k\mathrm{arccosh}(\lambda)} + \\
&+ b_1^* b_2 + b_2^* b_1 + |b_2|^2 e^{-2k\mathrm{arccosh}(\lambda)} \Big) - \frac{a^3}{3!} \Big(|b_1|^2 e^{2k\mathrm{arccosh}(\lambda)} + b_1^* b_2 - b_2^* b_1 - \\
&- \left. |b_2|^2 e^{-2k\mathrm{arccosh}(\lambda)} \Big) \left(e^{-\mathrm{arccosh}(\lambda)} - e^{\mathrm{arccosh}(\lambda)} \right)^3 + \ldots \Big] \right| .
\end{aligned}
$$

The even numbered and the odd numbered terms inside the square brackets in (3.31) can be collected under two different summations over the dummy index n

$$
\begin{aligned}
T = \Bigg| \left(\frac{i2mN\mu_0^2}{\hbar} \right) \int_0^\infty da \Bigg\{ & \sum_k \Big(|b_1|^2 e^{2k\mathrm{arccosh}(\lambda)} + b_1^* b_2 + b_2^* b_1 + |b_2|^2 e^{-2k\mathrm{arccosh}(\lambda)} \Big) \\
& \times \sum_{n=0}^{\infty} \Big[\frac{(-a)^{2n} (e^{-\mathrm{arccosh}(\lambda)} - e^{\mathrm{arccosh}(\lambda)})^{2n}}{(2n)!} \Big] + \\
& \sum_k \Big(|b_1|^2 e^{2k\mathrm{arccosh}(\lambda)} + b_1^* b_2 - b_2^* b_1 - |b_2|^2 e^{-2k\mathrm{arccosh}(\lambda)} \Big) \\
& \times \sum_{n=0}^{\infty} \Big[\frac{(-a)^{2n+1} (e^{-\mathrm{arccosh}(\lambda)} - e^{\mathrm{arccosh}(\lambda)})^{2n+1}}{(2n+1)!} \Big] \Bigg\} \Bigg| .
\end{aligned} \qquad (3.32)
$$

If we notice the fact that $(e^{-\mathrm{arccosh}(\lambda)} - e^{\mathrm{arccosh}(\lambda)}) = -2\sinh(\mathrm{arccosh}(\lambda))$ we can write (3.32) as

$$
\begin{aligned}
T = \Bigg| \left(\frac{i2mN\mu_0^2}{\hbar} \right) \int_0^\infty da \Bigg\{ & \sum_k \Big(|b_1|^2 e^{2k\mathrm{arccosh}(\lambda)} + b_1^* b_2 + b_2^* b_1 + |b_2|^2 e^{-2k\mathrm{arccosh}(\lambda)} \Big) \\
& \times \sum_{n=0}^{\infty} \left[\frac{\Big(2a \sinh(\mathrm{arccosh}\lambda) \Big)^{2\mathrm{n}}}{(2n)!} \right] + \\
& \sum_k \Big(|b_1|^2 e^{2k\mathrm{arccosh}(\lambda)} + b_1^* b_2 - b_2^* b_1 - |b_2|^2 e^{-2k\mathrm{arccosh}(\lambda)} \Big) \\
& \times \sum_{n=0}^{\infty} \left[\frac{\Big(2a \sinh(\mathrm{arccosh}\lambda) \Big)^{2\mathrm{n}+1}}{(2n+1)!} \right] \Bigg\} \Bigg| .
\end{aligned} \qquad (3.33)
$$

Since $\sinh(\text{arccosh}\lambda) = \sqrt{\lambda^2-1}$ this equation is equivalent to

$$T = \left| \left(\frac{i2mN\mu_0^2}{\hbar} \right) \int_0^\infty da \Bigg\{ \sum_k \left(|b_1|^2 e^{2k\text{arccosh}(\lambda)} + b_1^* b_2 + b_2^* b_1 + |b_2|^2 e^{-2k\text{arccosh}(\lambda)} \right) \times \sum_{n=0}^{\infty} \left[\frac{\left(2a\sqrt{\lambda^2-1} \right)^{2n}}{(2n)!} \right] + \sum_k \left(|b_1|^2 e^{2k\text{arccosh}(\lambda)} + b_1^* b_2 - b_2^* b_1 - |b_2|^2 e^{-2k\text{arccosh}(\lambda)} \right) \times \sum_{n=0}^{\infty} \left[\frac{\left(2a\sqrt{\lambda^2-1} \right)^{2n+1}}{(2n+1)!} \right] \Bigg\} \right|. \tag{3.34}$$

The two summations over the dummy index *n* in the first and second terms of this equation are equal to $\cosh(2a\sqrt{\lambda^2-1})$ and $\sinh(2a\sqrt{\lambda^2-1})$, respectively. After collecting the terms, (3.34) takes the following form:

$$T = \left| \left(\frac{i2mN\mu_0^2}{\hbar} \right) \int_0^\infty da \Bigg\{ \sum_k \left(|b_1|^2 e^{2k\text{arccosh}(\lambda)} + b_1^* b_2 \right) \times \left(\cosh(2a\sqrt{\lambda^2-1}) + \sinh(2a\sqrt{\lambda^2-1}) \right) + \sum_k \left(b_2^* b_1 + |b_2|^2 e^{-2k\text{arccosh}(\lambda)} \right) \times \left(\cosh(2a\sqrt{\lambda^2-1}) - \sinh(2a\sqrt{\lambda^2-1}) \right) \Bigg| \right|. \tag{3.35}$$

Realizing the fact that

$$\left(\cosh(2a\sqrt{\lambda^2-1}) + \sinh(2a\sqrt{\lambda^2-1}) \right) = e^{2a\sqrt{\lambda^2-1}} \quad and \tag{3.36}$$

$$\left(\cosh(2a\sqrt{\lambda^2-1}) - \sinh(2a\sqrt{\lambda^2-1}) \right) = e^{-2a\sqrt{\lambda^2-1}} \tag{3.37}$$

we arrive at (3.38) below.

$$T = \left| \left(\frac{i2mN\mu_0^2}{\hbar} \right) \int_0^\infty da \quad \Bigg\{ \quad \sum_k \left(b_2^* b_1 + |b_2|^2 e^{-2k\text{arccosh}(\lambda)} \right) e^{-2a\sqrt{\lambda^2-1}} + \sum_k \left(|b_1|^2 e^{2k\text{arccosh}(\lambda)} + b_1^* b_2 \right) e^{2a\sqrt{\lambda^2-1}} \Bigg\} \right|. \tag{3.38}$$

The reader with a keen eye may have already noticed that the second exponential integral in (3.38) diverges. We will omit the diverging second term of this equation on the physical grounds that ($a \to \infty$) corresponds to the zero momentum states and zero momentum inside the barrier amounts to no tunneling and hence to infinite tunneling time. To make this point

clearer, one should revisit (3.4) and then realize that it is practically $\frac{1}{\hat{p}} = \int_0^{a_{max}} e^{-a\hat{p}} \quad da$ and inserting $\hat{p} = 0$ in this equation corresponds to $a_{max} = \infty$. Since a zero momentum particle does not tunnel through the barrier we can safely omit divergent parts of the tunneling time expression corresponding to those states. After these comments, the equation we end up with is

$$T = \left| \left(\frac{i2mN\mu_0^2}{\hbar} \right) \int_0^{\infty} e^{-2a\sqrt{\lambda^2-1}} \quad da \left\{ \sum_{k=0}^{N} \left(b_2^* b_1 + |b_2|^2 e^{-2k\text{arccosh}(\lambda)} \right) \right\} \right|. \tag{3.39}$$

After taking the integral and doing the summation this equation becomes;

$$T = \left| \left(\frac{i2mN\mu_0^2}{\hbar} \right) \left(\frac{1}{2\sqrt{\lambda^2-1}} \right) \left\{ \left(b_2^* b_1 \right) (1+N) + |b_2|^2 \frac{\left(e^{2\text{arccosh}(\lambda)} - e^{-2N\text{arccosh}(\lambda)} \right)}{\left(e^{2\text{arccosh}(\lambda)} - 1 \right)} \right\} \right|. \tag{3.40}$$

The next steps are calculating $b_2^* b_1$ and $|b_2|^2$ using (2.80) and (2.81). From (2.81) we have

$$b_2^* = \left(c_1^* e^{-iN\arccos(\varepsilon)} \right) \frac{\left(2e^{(N+1)\text{arccosh}(\lambda)} - e^{-i\arccos(\varepsilon)+(N+1)\text{arccosh}(\lambda)} - e^{N\text{arccosh}(\lambda)} \right)}{\left(e^{2\text{arccosh}(\lambda)} - 1 \right)}. \tag{3.41}$$

Multiplying this with (2.80) we get the first desired result

$$\begin{aligned} b_2^* b_1 = \frac{|c_1|^2}{\left(e^{2\text{arccosh}(\lambda)} - 1 \right)^2} \Big\{ & 2e^{3\text{arccosh}(\lambda)} - 6e^{2\text{arccosh}(\lambda)} + 2e^{i\arccos(\varepsilon)+2\text{arccosh}(\lambda)} \\ & - e^{-i\arccos(\varepsilon)+3\text{arccosh}(\lambda)} + 2e^{-i\arccos(\varepsilon)+2\text{arccosh}(\lambda)} + 2e^{\text{arccosh}(\lambda)} - e^{i\arccos(\varepsilon)+\text{arccosh}(\lambda)} \Big\}. \end{aligned} \tag{3.42}$$

From (3.41) and (2.81) we obtain

$$\begin{aligned} |b_2|^2 = \frac{|c_1|^2}{\left(e^{2\text{arccosh}(\lambda)} - 1 \right)^2} \Big\{ & 5e^{(2N+2))\text{arccosh}(\lambda)} - 2e^{i\arccos(\varepsilon)+(2N+2)\text{arccosh}(\lambda)} \\ & - 4e^{(2N+1)\text{arccosh}(\lambda)} - 2e^{-i\arccos(\varepsilon)+(2N+2)\text{arccosh}(\lambda)} + e^{-i\arccos(\varepsilon)+(2N+1)\text{arccosh}(\lambda)} \\ & + e^{i\arccos(\varepsilon)+(2N+1)\text{arccosh}(\lambda)} + e^{2N\text{arccosh}(\lambda)} \Big\}. \end{aligned} \tag{3.43}$$

After plugging (3.42) and (3.43) into (3.40) and expressing N in terms of the barrier width

we end up with

$$T = \left| \left(\frac{i2mL\mu_0}{\hbar} \right) \left(\frac{1}{2\sqrt{\lambda^2-1}} \right) \frac{|c_1|^2}{\left(e^{2\mathrm{arccosh}(\lambda)}-1\right)^2} \left\{ \left(1+\frac{L}{\mu_0}\right) \left\{ 2e^{3\mathrm{arccosh}(\lambda)} \right.\right.\right.$$
$$- 6e^{2\mathrm{arccosh}(\lambda)} + 2e^{i\arccos(\varepsilon)+2\mathrm{arccosh}(\lambda)} - e^{-i\arccos(\varepsilon)+3\mathrm{arccosh}(\lambda)} + 2e^{-i\arccos(\varepsilon)+2\mathrm{arccosh}(\lambda)}$$
$$\left.\left. + 2e^{\mathrm{arccosh}(\lambda)} - e^{i\arccos(\varepsilon)+\mathrm{arccosh}(\lambda)} \right\} + \left\{ 5e^{(2N+2))\mathrm{arccosh}(\lambda)} - 2e^{i\arccos(\varepsilon)+(2N+2)\mathrm{arccosh}(\lambda)} \right.\right.$$
$$- 4e^{(2N+1)\mathrm{arccosh}(\lambda)} - 2e^{-i\arccos(\varepsilon)+(2N+2)\mathrm{arccosh}(\lambda)} + e^{-i\arccos(\varepsilon)+(2N+1)\mathrm{arccosh}(\lambda)}$$
$$\left.\left.\left. + e^{i\arccos(\varepsilon)+(2N+1)\mathrm{arccosh}(\lambda)} + e^{2N\mathrm{arccosh}(\lambda)} \right\} \frac{\left(e^{2\mathrm{arccosh}(\lambda)} - e^{-2N\mathrm{arccosh}(\lambda)}\right)}{\left(e^{2\mathrm{arccosh}(\lambda)}-1\right)} \right\} \right|. \tag{3.44}$$

The last step is inserting the relevant expressions for λ and ε in (3.44) . The explicit forms of these two parameters are, as we have stated before, $\lambda = \left(1 - \frac{m(E-V_0)\mu_0^2}{\hbar^2}\right)$ and $\varepsilon = \left(1 - \frac{mE\mu_0^2}{\hbar^2}\right)$.

3.2. Introduction to the Quantum Zeno and Anti-Zeno Effects

The quantum Zeno effect is named after the Greek sophist philosopher Zeno of Elea who was born about 488 BC in Elea, a small town now in northern Italy. Zeno was known to be the most brilliant disciple of Parmenides who was a very prominent figure of the Eleatic school of philosophy. According to this school of thought, the senses were deceptive, all appearances of motion, change and multiplicity were mere illusions; there was only one truth that was static and could not be decomposed into parts. It was therefore indivisible and did not develop. This view was in strict contrast with the notion of reality of Pythagoras and Heraclitus, that defended the world of changes and becoming. That's why Parmenides' views were ridiculed by his contemporaries and as a result Zeno elaborated a number of paradoxes to defend Eleatic system of thought and attack then existing common conceptions about space and time. Here, we will mention three of the most famous of these paradoxes of motion.

The Dichotomy paradox states that *"there is no motion, because that which is moved must arrive at the middle before it arrives at the end, and so on ad infinitum."* Let us restate this paradox in more general terms. Imagine that someone tries to go from point A to point B. Before he can cover half the distance to the end, he must cover the first quarter. Before this, he must cover the first eight and before that the first sixteenth and so on ad

infinitum. This means that before one can cover any distance at all he must cover an infinite number of smaller parts. The argument of Zeno was that covering these infinite number of parts in a finite time interval would be impossible. Thus Zeno concluded that the motion can never get started. But the common knowledge is on the contrary, for everything around us is seen to be on the move. Thus, the argument inevitably leads us to conclude that all motion is an illusion. This paradox is called Dichotomy because it involves repeatedly dividing the distances into two separate parts. But what is paradoxical about Zeno's argument? He says that any movement can be subdivided into an infinite number of ever decreasing steps. This is not by itself paradoxical if we take the infinite divisibility of space and time for granted even though this is not an experimentally confirmed fact as yet. What is paradoxical here, is that you need to perform an infinite number of tasks in a finite time interval so as to accomplish a supertask, i.e. going from point A to point B. Our intuition tells us that it is impossible for finite beings to manage infinite number of tasks in a finite time.

The fist attempt to resolve this paradox came from Aristotle by distinguishing potential and actual infinities. He said, if the infinite units of time or space that one needs to pass in order to accomplish a super task are actual the supertask is not manageable, if the units are potential it is possible. According to this position Zeno's infinite subdivision of motion is purely mathematical but even if we accept this point it is necessary to confirm that mathematically it is possible to handle infinities in a coherent way. But at the time of Aristotle the mathematical tools for this were nonexistent. Today, we can say that Dichotomy is not paradoxical.

Achilles and the Tortoise is a symmetric counterpart of Dichotomy. Achilles has to race a tortoise, the tortoise is given a head start. The argument is that Achilles could never catch up with the tortoise because he must first reach where the tortoise started, by this time the tortoise has crawled up an additional distance. Thus, whenever Achilles reaches the position previously occupied by the tortoise, the tortoise would have moved on ahead. Zeno argues that for Achilles to reach the tortoise he must perform an infinite sum of time or spacial increments. If space and time are continuous, an infinite sum of elements tending towards zero length or duration must have a total of zero length or duration. Alternatively, if space and time are discrete, then an infinite sum of finite elements must be of infinite length. Since Achilles is seen to overtake the tortoise, the above arguments fail. Thus we are led to conclude that both space and time can neither

be continuous nor discrete. This forces us to consider that space and time are illusions.

A Flying Arrow is at rest. Imagine an arrow flying through space. Time is considered to be made up of instants. These instants are defined as the smallest measure and they are indivisible. At any instant the arrow is observed, it is seen to occupy a space equal to its length. If the arrow is seen to move, the observer can divide an instant into a time when the arrow was here and a time when the arrow was there. This would mean that the instant of time consists of smaller parts, which is a direct violation of the definition of the instant as being indivisible. Thus, Zeno asserts that there are no instants of time when the arrow is in motion and this leads to the conclusion that the arrow is always at rest and that all motion is illusory.

It is fairly reasonable to say that the paradoxes of Zeno stem from human efforts to comprehend the infinities. Although unwarranted as yet, the infinite divisibility of space-time is now mathematically coherent. But still, Zeno's paradoxes contain some other physical premises that also require careful consideration. The Achilles and Tortoise paradox mentioned above assumes some observational procedure. It requires to check the positions of Achilles and the tortoise in the beginning of the race then again when Achilles reaches the position the tortoise occupied at the previous step, and finally repeat observing the positions of the contenders at each step. As it is seen, this procedure assumes that it is possible to perform position measurements on the system at will. But in the world of quanta the question comes to ones mind as to the effects of these measurements on the system and whether it is possible to make infinitely frequent measurements taken for granted by Zeno.

The quantum Zeno effect is the inhibition of transitions between quantum states by frequent measurements and this term was first used by Misra and Sudarshan in a 1977 paper which blends rigorous mathematics with subtle and often ironical remarks about philosophy and cats. The system that they considered in their paper was an unstable particle like a radioactive nucleus which in classical statistical mechanics is treated heuristically and the exponential decay law

$$N(t) = N(t_0)e^{-\lambda(t-t_0)} \tag{3.45}$$

is obtained. Here $N(t)$ is the number of nuclei that have not yet decayed and the only assumption is that the probability of decay per unit time is proportional to the existing number of nuclei.

While the decay of quantum mechanical systems are expected to be similar to this classical model of decay, theoretical studies proposed that for very short and very long time

scales during the decay there should be deviations from the exponential behavior. In the short time regimes as measured from the time of preparation of the state of the the system we see the manifestations of the quantum Zeno effect.

There are a number of alternative arguments to support the claim that there is a quadratic region for short time scales in the survival probability that ultimately gives rise to the quantum Zeno effect.

The first argument that supports the initial-time non-exponential decay claim is rooted in the generalised uncertainty principle. The argument starts from the well known mathematical inequality

$$\Delta A \Delta B \geq \frac{1}{2}|\langle [A, B]\rangle|, \tag{3.46}$$

where ΔA and ΔB are the uncertainties of the observables A and B respectively. From now on, we will use the Hamiltonian of the decaying system in place of the observable B. First thing to realize is the fact that

$$\langle [A, H]\rangle = i\hbar \frac{d\langle A\rangle}{dt}. \tag{3.47}$$

Combining (3.47) with (3.46) we get

$$\Delta A \geq \frac{\hbar}{2\Delta E}\left|\frac{d\langle A\rangle}{dt}\right|. \tag{3.48}$$

If we use the projection to the undecayed initial state as the operator A that has appeared above, i.e. $A = |\psi_0\rangle\langle\psi_0|$, where ψ_0 is the initial unstable state of the system; we can write the survival probability as

$$P(t) = |\langle\psi_0|\psi(t)\rangle|^2 = \langle A\rangle = \langle A^2\rangle, \tag{3.49}$$

where $|\psi(t)\rangle = e^{-\frac{iH}{\hbar}t}|\psi_0\rangle$. Using (3.49) we can write the standard deviation of A as

$$(\Delta A)^2 = \langle A^2\rangle - \langle A\rangle^2 = P - P^2. \tag{3.50}$$

Using this result in (3.48) we have

$$\sqrt{P(1-P)} \geq \frac{\hbar}{2\Delta E}\left|\frac{dP(t)}{dt}\right|. \tag{3.51}$$

At $t = 0$ the survival probability must be one by definition hence the left-hand side of (3.51) is zero at $t = 0$ and this forces the right-hand side to become zero as well. This leads to the conclusion that the derivative of the survival probability is zero at $t = 0$. This in tern tells us that the survival probability must not have any term linear in time, because if it did the derivative of the survival probability at $t = 0$ would be non-zero. The final conclusion that

is drawn from all this is that the survival probability is non-exponential and quadratic at the initial stage of the decay. And this concludes the first argument for the quadratic decay claim at the initial stage of decay.

The second argument follows directly from wave mechanics and goes like this: First of all, let us consider the decay of an unstable quantum system the initial undecayed state of which is represented by ψ_0 at $t = 0$. The state of the system at a later time t is called $\psi(t)$. The time evolution of the system is governed by the unitary operator $U(t)$, where

$$U(t) = e^{-\frac{iH}{\hbar}t}. \tag{3.52}$$

The time evolved state is then obtained by

$$|\psi(t)\rangle = U(t)|\psi_0\rangle, \tag{3.53}$$

where H is the Hamiltonian of the system, which is assumed to be time independent. For the following discussion we will assume that all functions are sufficiently regular to admit series expansions. Having said that, now if we expand (3.52) as

$$e^{-\frac{iH}{\hbar}t} \approx \left(1 - \frac{iH}{\hbar}t - \frac{H^2}{2\hbar^2}t^2\right), \tag{3.54}$$

we obtain the time evolved state using (3.53) and it reads

$$|\psi(t)\rangle \approx \left(1 - \frac{iH}{\hbar}t - \frac{H^2}{2\hbar^2}t^2\right)|\psi_0\rangle. \tag{3.55}$$

According to the wave function collapse theory of measurements, any observation that the state has not decayed will cause a collapse of the wave function to the undecayed state. The survival amplitude is defined as

$$A(t) = \langle\psi_0|\psi(t)\rangle, \tag{3.56}$$

and the survival probability, the probability that the state has not decayed, is the modulus squared of this amplitude,i.e.

$$P(t) = |\langle\psi_0|\psi(t)\rangle|^2. \tag{3.57}$$

Using (3.53), (3.57) is equal to

$$P(t) = |\langle\psi_0|U(t)|\psi_0\rangle|^2. \tag{3.58}$$

Plugging (3.54) into (3.58) the survival probability takes the form

$$P(t) \approx 1 - \frac{t^2}{\hbar^2}\left(\langle\psi_0|H^2|\psi_0\rangle - \langle\psi_0|H|\psi_0\rangle^2\right). \tag{3.59}$$

Letting

$$(\Delta E)^2 = \langle\psi_0|H^2|\psi_0\rangle - \langle\psi_0|H|\psi_0\rangle^2, \tag{3.60}$$

the survival probability in the short time limit can be written as

$$P(t) \approx 1 - \frac{t^2}{\hbar^2}(\Delta E)^2 . \tag{3.61}$$

If we define $\tau_z = \frac{1}{\Delta E}$ as the Zeno Time, (3.61) leads to

$$P(t) \approx 1 - \frac{t^2}{\hbar^2 \tau_z^2} . \tag{3.62}$$

What (3.62) conveys is that, the short-time decay is not exponential but quadratic.

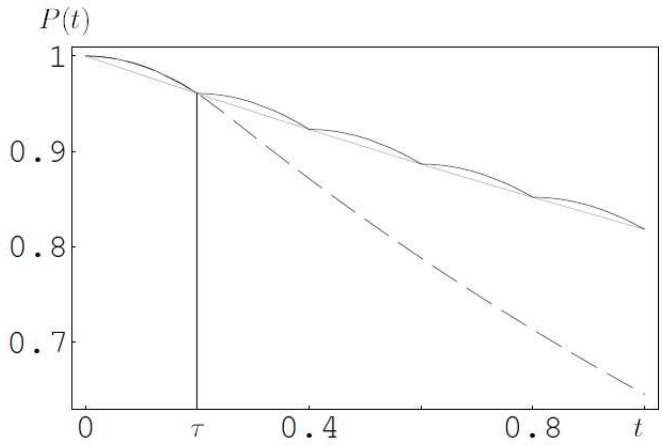

Figure 3.1. Quantum Zeno effect illustrated for a system which is subjected to five consecutive von Neuman projections in one second. *This figure is from the review [22] by Saverio Pascazio.*

Now, let's see how this short-time quadratic decay region can be exploited to inhibit the decay of an unstable quantum system. If we assume that one measures the systems state n times during a time interval t, the survival probability at the end of this whole process is equal to

$$[P(t)]^n = \left(1 - \frac{t^2}{\hbar^2 \tau_z^2 n^2}\right)^n . \tag{3.63}$$

In the limit of continuous measurements, i.e. $n \to \infty$, this probability goes to one because

$$ln\left(1 - \frac{t^2}{\hbar^2 \tau_z^2 n^2}\right)^n \to 0. \tag{3.64}$$

This is the Quantum Zeno Effect (QZE) and it is a consequence of the short-time behavior of the quantum mechanical evolution law. The mathematical feature of the Schrödinger

equation is such that in a short time of the order of $1/n$, the phase of the wave function evolves like $O(1/n)$ where as the probability changes like $O(1/n^2)$ and in the limit $n \to \infty$ the survival probability goes to one. What it means is that if we conduct continuous observations on an unstable quantum system, the system never has a chance to decay. This is much like the flying arrow paradox of Zeno of Elea that we mentioned before. There a flying arrow which is continuously observed during its flight seems to be motionless and here in the quantum Zeno effect a continuously measured system is inhibited from decaying and seems as if its stuck to the initial state and does not evolve at all. We can say that Zeno's quantum mechanical arrow, i.e. the wave function, sped by the Hamiltonian, does not move if it is continuously observed.

The evolution of a system which is subjected to $n = 5$ consecutive measurements in one second is depicted in the Figure 3.1. The undisturbed system follows the dashed curve after the short-time quadratic region whereas measurements conducted on the system in $0.2s$ intervals force the system to follow the full line. In the limit of continuous observations the survival probability approaches one.

Up to this point in this section, we have stated, using two different arguments, that there exists a short-time quadratic region in the survival probability of an unstable state. But that is not the whole story, the evolution of an unstable quantum system is actually characterized by three distinct regimes one of which is the aforementioned quadratic region. The other two of these regimes are the intermediate one during which the familiar exponential law of decay sets in and the long-time regime which is governed by some form of power-law. These regimes are marked in the Figure 3.2 [1].

Close inspection of Figure 3.2 reveals a damped oscillatory transition between the initial quadratic slow-decay period and the intermediate exponential regime. At that point a steep drop in the survival probability is observed immediately after the Zeno time. It is expected therefore that interfering with a transition at this steep drop period of evolution causes the decay to accelerate rather than slow down. Frequent interruptions at this stage collapse the wave function every time to the initial state and therefore force the system to repeat the initial period of fast decay again and again after each measurement. This phenomenon is called the Quantum Anti-Zeno effect (AZE).

The short-time quadratic regime of the quantum mechanical evolution, which is the main driving force behind the QZE, is quite general but not universal. The experimental difficulty is that the quadratic time dependence takes place usually at very short times for

[1] This figure is from the review [22] by Saverio Pascazio.

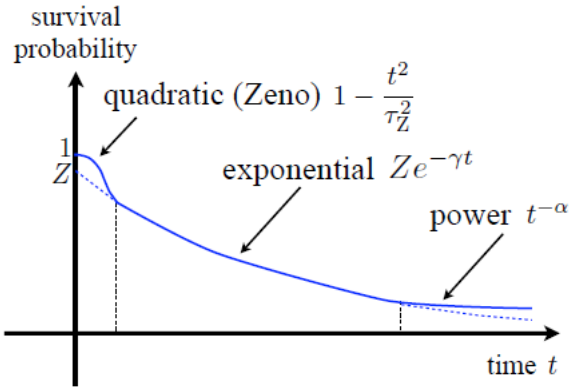

Figure 3.2. Survival probability of an unstable state. The three distinct regimes of quantal evolution are marked. *This figure is from the review [22] by Saverio Pascazio.*

genuine unstable systems, i.e. their Zeno-time is usually very small. Nevertheless contemporary experimental techniques enable physicists to prepare artificial unstable systems whose Zeno-time is long enough to inspect QZE and AZE . In experiment [39] ultra-cold sodium atoms were trapped in a periodic optical potential and the number of atoms that remained inside the barrier was measured as a function of the duration of tunneling. Figure 3.3 beautifully depicts QZE. The hollow squares in the figure represent the survival probability for the uninterrupted decay whereas the solid circles represent the situation in the case of frequent measurements. A much slower decay trend is evident from the figure compared to the natural decay and this is a dramatic manifestation of QZE.

Quantum Anti-Zeno effect is also demonstrated in the same experiment, i.e. [39], and Figure 3.4 is the result that they had. Again the solid circles in this figure show the evolution of the unstable system that has been the subject of frequent measurements and the hollow squares represent the uninterrupted decay. As the reader can see the decay rate is significantly increased by frequent observations compared to the natural decay.

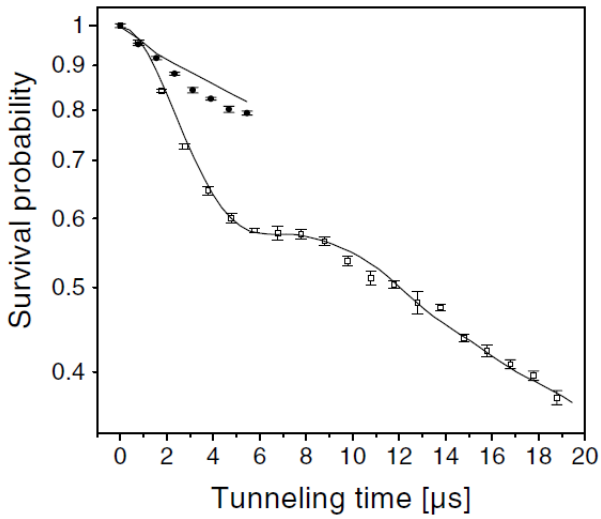

Figure 3.3. Observation of the Quantum Zeno effect in the experiment [39].

3.3. Quantum Zeno and Anti-Zeno Effects in Polymer Representation

In the previous section we have gone over the basics of QZE and AZE. The next concept that we want to consider is the relation of our tunneling time expression , i.e. (3.44), to the quantum Zeno effect. In our work, the tunneling particle constitutes an unstable system and one may expect to observe Quantum Zeno and anti-Zeno effects through the change in the tunneling times as we change the characteristic length scale μ_0. Altering the characteristic length scale amounts to altering the frequency of position measurements therefore changing the number of discrete steps the particle takes inside the barrier should effect the tunneling time in accordance with the Quantum Zeno and anti-Zeno effects. We did a numerical analysis on our tunneling time expression, i.e. (3.44), to see if it accords with QZE and AZE proposals made above. In that analysis, we expanded (3.44) in a Maclaurin Series in μ_0 since it exquisitely depends on it. We have used $L = 1nm$ as the barrier width, the tunneling particle is taken to be an electron, the height of the potential is taken to be $9.7eV$ and the energy of the electron $5.5eV$. The following figure , i.e. Figure 3.5, is the result of this analysis. Close inspection of that figure reveals that as we decrease the characteristic length scale μ_0, i.e. increase the frequency of position measurements, tunneling time decreases up to a point and then as we continue to even smaller length scales the tunneling time displays a dramatic increase. Tunneling time takes a minimum value of $2\, femto\, seconds$ when $\mu_0 = 5.8 \times 10^{-11} m$ hence it is consistent with some of the experiments in the literature

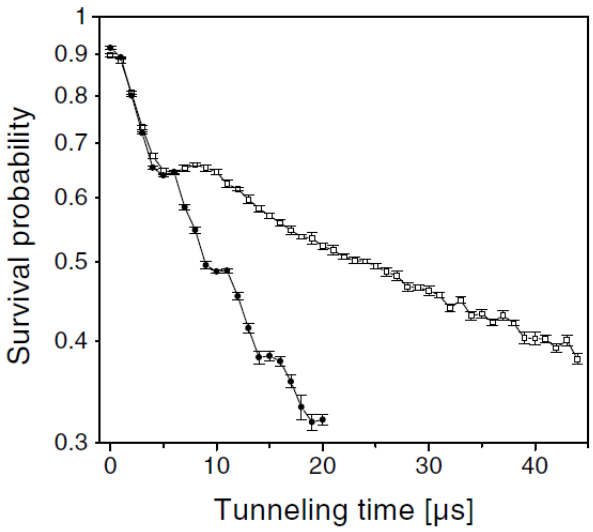

Figure 3.4. Observation of the Quantum Anti-Zeno effect in the experiment [39].

although the potentials that are used in those experiments do not have simple rectangular profiles. We may interpret the part of the tunneling time curve that descends as we decrease μ_0 as the anti-Zeno region and the other part where the tunneling time increases dramatically can be coined the Zeno region.

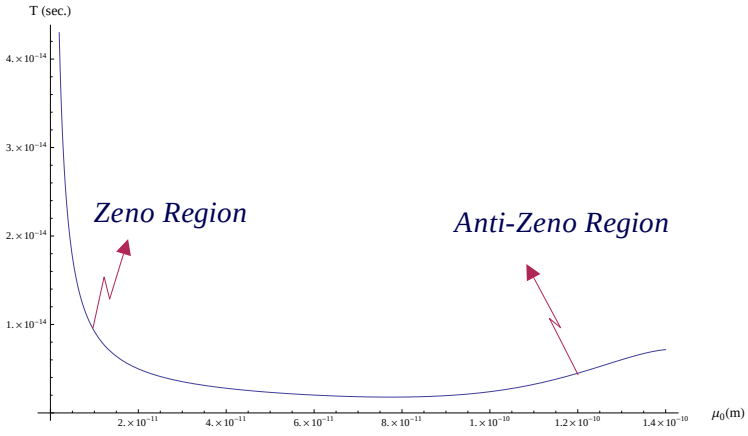

Figure 3.5. Tunneling time against polymeric length scale. Discretization of position leads to Zeno effect.

Taking the numerical analysis a step further we wanted to see the behaviour of the reflection and transmission coefficients with respect to the change in the characteristic length scale μ_0. For this purpose, we used the same numerical values for the tunneling particle that we used to obtain figure 3.5, and we got the following graphs, i.e. figures 3.6 and 3.7, for the

reflection and transmission coefficients.

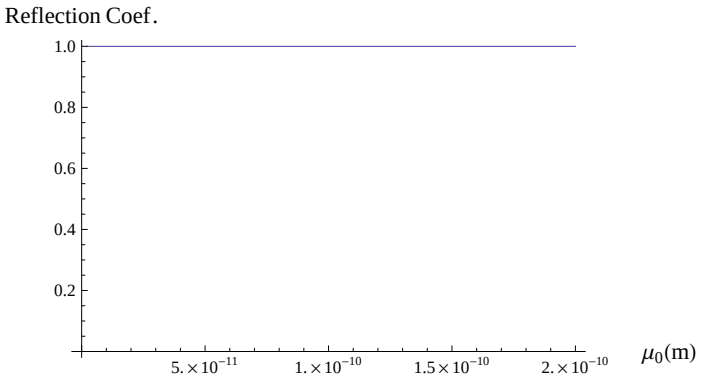

Figure 3.6. Reflection coefficient against polymeric length scale.

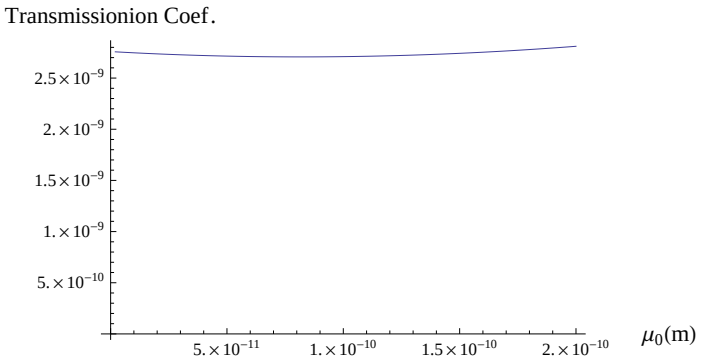

Figure 3.7. Transmission coefficient against polymeric length scale.

Inspection of these graphs reveals that the transmission coefficient is only a minute fraction of the whole probability hence most of the incoming plane wave which is representing the particle is reflected back and this is in accordance with the long tunneling times that we have seen in figure 3.5.

CHAPTER 4

CONCLUSIONS

We applied the polymer quantization formalism to the well known quantum tunneling phenomenon in order to see if it is possible to get sensible results similar to Schrödinger formulation. For this purpose, we made use of a non-relativistic quantum particle in one dimension tunneling through a rectangular potential barrier. Since there is no counterpart to the Schrödinger momentum operator in this scheme we had to introduce a new one in terms of shifting operator $\hat{V}(\mu)$. After regularizing the Hamiltonian using this operator, the eigenvalue equations pertaining to different regions of the potential turned into second order difference equations. Solutions of these gave us the wave functions. Conserving the probability current led to the four unknown coefficients out of the five. And then, the transmission and reflection coefficients were calculated and their sum, which is a consistency check on the formalism, was seen to be one as expected. Then, we defined a differential time operator to calculate the time it takes a non-relativistic particle to tunnel through the barrier. We calculated the tunneling time as the expectation value of the finite time operator, which is the integral of differential time operator between the boundaries of the barrier. Our calculations revealed that the tunneling time expression we got complies with the predictions of Quantum Zeno and anti-Zeno effects. The variation of the tunneling time with the fundamental length scale of polymer quantization reveals that as we decrease the length scale, thereby increase the discrete position steps that the particle takes and in a sense increase the number of position measurements made on the particle, the tunneling time first decreases up to a point and then as we continue to further decrease the length scale the tunneling time starts to increase dramatically. The part of the tunneling time curve to the right of the minimum of the curve can be identified with the behaviour inline with the Quantum anti-Zeno effect and the part to left can be coined the Quantum Zeno region.

REFERENCES

[1] Abhay Ashtekar and Jerzy Lewandowski. Relation between polymer and fock excitations. *Classical and Quantum Gravity*, 18(18):L117, 2001.

[2] Abhay Ashtekar, Stephen Fairhurst, and Joshua L. Willis. Quantum gravity, shadow states and quantum mechanics. *Classical and Quantum Gravity*, 20(6):1031, 2003. arXiv:gr-qc/0207106v3.

[3] Klaus Fredenhagen and Felix Reszewski. Polymer state approximation of schrödinger wavefunctions. *Classical and Quantum Gravity*, 23(22):6577, 2006. arXiv:gr-qc/0606090v2.

[4] Sanjeev S. Seahra, Iain A. Brown, Golam Mortuza Hossain, and Viqar Husain. Primordial polymer perturbations. arXiv:1207.6714v2 [astro-ph.CO].

[5] Andreas Kreienbuehl and Tomasz Pawłowski. Singularity resolution from polymer quantum matter. *Phys. Rev. D*, 88:043504, Aug 2013. arXiv:1302.6566v2 [gr-qc].

[6] J M Velhinho. The quantum configuration space of loop quantum cosmology. *Classical and Quantum Gravity*, 24(14):3745, 2007. arXiv:0704.2397v2 [gr-qc].

[7] Golam Mortuza Hossain, Viqar Husain, and Sanjeev S. Seahra. Propagator in polymer quantum field theory. *Phys. Rev. D*, 82:124032, Dec 2010.

[8] J. Fernando Barbero G., Jorge Prieto, and Eduardo J. S. Villaseñor. Band structure in the polymer quantization of the harmonic oscillator. *Classical and Quantum Gravity*, 30(16):165011, 2013. arXiv:1305.5406v1 [gr-qc].

[9] Dah-Wei Chiou. Galileo symmetries in polymer particle representation. *Classical and Quantum Gravity*, 24(10):2603, 2007. arXiv:gr-qc/0612155v3.

[10] Alejandro Corichi, Tatjana Vukašinac, and José A. Zapata. Polymer quantum mechanics and its continuum limit. *Phys. Rev. D*, 76:044016, Aug 2007. arXiv:0704.0007v2 [gr-

qc].

[11] Alejandro Corichi, Tatjana Vukašinac, and José A. Zapata. Hamiltonian and physical hilbert space in polymer quantum mechanics. *Classical and Quantum Gravity*, 24(6):1495, 2007. arXiv:gr-qc/0610072v2.

[12] Viqar Husain, Jorma Louko, and Oliver Winkler. Quantum gravity and the coulomb potential. *Phys. Rev. D*, 76:084002, Oct 2007. arXiv:0707.0273v2.

[13] Gabor Kunstatter, Jorma Louko, and Jonathan Ziprick. Polymer quantization, singularity resolution, and the $1/r^2$ potential. *Phys. Rev. A*, 79:032104, Mar 2009. arXiv:0809.5098v2.

[14] Golam Mortuza Hossain, Viqar Husain, and Sanjeev S. Seahra. Background-independent quantization and the uncertainty principle. *Classical and Quantum Gravity*, 27(16):165013, 2010. arXiv:1003.2207v1 [gr-qc].

[15] Guillermo Chacón-Acosta, Elisa Manrique, Leonardo Dagdug, and Hugo A. Morales-Técotl. Statistical thermodynamics of polymer quantum systems. *SIGMA*, 7:110, 2011. arXiv:1109.0803v2 [gr-qc].

[16] Elías Castellanos and Guillermo Chacón-Acosta. Polymer bose–einstein condensates. arXiv:1301.5362v1 [gr-qc].

[17] Tommaso F. Demarie and Daniel R. Terno. Entropy and entanglement in polymer quantization. *Classical and Quantum Gravity*, 30(13):135006, 2013. arXiv:1209.3087v2 [gr-qc].

[18] E. U. Condon and P. M. Morse. Quantum mechanics of collision processes i. scattering of particles in a definite force field. *Rev. Mod. Phys.*, 3:43–88, Jan 1931.

[19] L. A. MacColl. Note on the transmission and reflection of wave packets by potential barriers. *Phys. Rev.*, 40:621–626, May 1932.

[20] Wolfgang Pauli. *Handbuch der Physik*, volume 24. Springer, Berlin, 1933.

[21] Durmuş Ali Demir. Real-time tunneling. arXiv:quant-ph/9809036v2.

[22] Saverio Pascazio. All you ever wanted to know about the quantum zeno effect in 70 minutes. *Open Systems & Information Dynamics*, 21(01n02):1440007, 2014. arXiv:1311.6645v1 [quant-ph].

[23] P. Facchi and S. Pascazio. Quantum zeno dynamics: mathematical and physical aspects. *J. Phys. A*, 41(49):493001, 2008. arXiv:0903.3297v1 [math-ph].

[24] Anu Venugopalan. The quantum zeno effect watched pots in the quantum world. *Resonance*, 12(4):52–68, 2007. arXiv:1211.3498v1 [physics.hist-ph].

[25] Orly Alter and Yoshihisa Yamamoto. Quantum zeno effect and the impossibility of determining the quantum state of a single system. *Phys. Rev. A*, 55:R2499–R2502, Apr 1997.

[26] A.S. Sanz, C. Sanz-Sanz, T. Gonzalez-Lezana, O. Roncero, and S. Miret-Artes. Quantum zeno effect: Quantum shuffling and markovianity. *Ann. Phys.*, 327(4):1277 – 1289, 2012. arXiv:1112.3829v2 [quant-ph].

[27] Paolo Facchi, Sandro Graffi, and Marilena Ligabò. The classical limit of the quantum zeno effect. *J. Phys. A*, 43(3):032001, 2010. arXiv:0911.5675v1 [quant-ph].

[28] Asher Peres. Zeno paradox in quantum theory. *Am. J. Phys.*, 48(11):931–932, 1980.

[29] Paolo Facchi and Marilena Ligabò. Quantum zeno effect and dynamics. *J. Math. Phys.*, 51(2):–, 2010. arXiv:0911.2201v1 [math-ph].

[30] B. Misra and E. C. G. Sudarshan. The zeno's paradox in quantum theory. *J. Math. Phys.*, 18(4):756–763, 1977.

[31] A. P. Balachandran and S. M. Roy. Quantum anti-zeno paradox. *Phys. Rev. Lett.*, 84:4019–4022, May 2000. arXiv:quant-ph/9909056v1.

[32] A. G. Kofman and G. Kurizki. Acceleration of quantum decay processes by frequent

observations. *Nature*, 405(6786):546–550, June 2000. arXiv:quant-ph/0102002v2.

[33] Steven R. Wilkinson, Cyrus F. Bharucha, Martin C. Fischer, Kirk W. Madison, Patrick R. Morrow, Qian Niu, Bala Sundaram, and Mark G. Raizen. Experimental evidence for non-exponential decay in quantum tunnelling. *Nature*, 387(6633):575–577, June 1997.

[34] Wayne M. Itano, D. J. Heinzen, J. J. Bollinger, and D. J. Wineland. Quantum zeno effect. *Phys. Rev. A*, 41:2295–2300, Mar 1990.

[35] Paul Kwiat, Harald Weinfurter, Thomas Herzog, Anton Zeilinger, and Mark A. Kasevich. Interaction-free measurement. *Phys. Rev. Lett.*, 74:4763–4766, Jun 1995.

[36] A. G. Kofman and G. Kurizki. Quantum zeno effect on atomic excitation decay in resonators. *Phys. Rev. A*, 54:R3750–R3753, Nov 1996.

[37] Wenqiang Zheng, D. Z. Xu, Xinhua Peng, Xianyi Zhou, Jiangfeng Du, and C. P. Sun. Experimental demonstration of the quantum zeno effect in nmr with entanglement-based measurements. *Phys. Rev. A*, 87:032112, Mar 2013.

[38] Janik Wolters, Max Strauß, Rolf Simon Schoenfeld, and Oliver Benson. Quantum zeno phenomenon on a single solid-state spin. *Phys. Rev. A*, 88:020101, Aug 2013. arXiv:1301.4544v2 [quant-ph].

[39] M. C. Fischer, B. Gutiérrez-Medina, and M. G. Raizen. Observation of the quantum zeno and anti-zeno effects in an unstable system. *Phys. Rev. Lett.*, 87:040402, Jul 2001.

[40] P. Facchi, H. Nakazato, and S. Pascazio. From the quantum zeno to the inverse quantum zeno effect. *Phys. Rev. Lett.*, 86:2699–2703, Mar 2001. arXiv:quant-ph/0006094v2.

[41] F. Strocchi. *An Introduction to the Mathematical Structure of Quantum Mechanics*, volume 27 of *Advanced Series in Mathematical Physics*. World Scientific Publishing Co. Pte. Ltd., 2005.

[42] F. Strocchi. *An Introduction to the Mathematical Structure of Quantum Mechanics*, vol-

ume 27 of *Advanced Series in Mathematical Physics*. World Scientific Publishing Co. Pte. Ltd., 2005.

[43] Hans Halvorson. Complementarity of representations in quantum mechanics. *Studies in History and Philosophy of Science Part B: Studies in History and Philosophy of Modern Physics*, 35(1):45 – 56, 2004. arXiv:quant-ph/0110102v1.

[44] Ernesto Flores-González, Hugo A. Morales-Técotl, and Juan D. Reyes. Propagators in polymer quantum mechanics. *Ann. Phys.*, 336(0):394 – 412, 2013. arXiv:1302.1906v1 [math-ph].

[45] Nouredine Zettili. *Quantum Mechanics*. John Wiley & Sons LTD., 2001.

[46] Bransden B. H. & Joachin C. J. *Quantum Mechanics*. Prentice Hall, 2nd edition, 2000.

APPENDIX A

SUPPLEMENTARY INFORMATION ON WEYL ALGEBRA

A.1. DERIVATIONS of MISCELLANEOUS RELATIONS

- *Derivation of* $\hat{W}(\zeta) = e^{\frac{i}{2}\lambda\mu}\hat{U}(\lambda)\hat{V}(\mu)$ *goes as follows:*

First of all, we note that $\hat{U}(\lambda) \equiv \hat{W}(\lambda d)$ and $\hat{V}(\mu) \equiv \hat{W}(i\frac{\mu}{d})$. Next, we insert these into (1.1) and get :

$$\hat{U}(\lambda)\hat{V}(\mu) = \hat{W}\Big(\lambda d\Big)\hat{W}\left(i\frac{\mu}{d}\right) = e^{\frac{i}{2}Im\left[\lambda d\,\overline{(i\frac{\mu}{d})}\right]}\hat{W}\left(\lambda d + i\frac{\mu}{d}\right) \tag{A.1}$$

which is equal to

$$\hat{U}(\lambda)\hat{V}(\mu) = e^{-\frac{i}{2}\lambda\mu}\hat{W}\left(\zeta\right) \tag{A.2}$$

from this we arrive at

$$\hat{W}\left(\zeta\right) = e^{\frac{i}{2}\lambda\mu}\hat{U}(\lambda)\hat{V}(\mu)\ . \tag{A.3}$$

- *Derivation of the Weyl commutation relations:*

1. We use (1.1) again and write

$$\hat{U}(\lambda_1)\hat{U}(\lambda_2) = e^{\frac{i}{2}Im\left[\lambda_1\overline{\lambda_2}\right]}\hat{U}\left(\lambda_1 + \lambda_2\right). \tag{A.4}$$

If we realize the fact that $Im\left[\lambda_1\overline{\lambda_2}\right] = 0$ since both λ_1 and λ_2 are real parameters, we obtain

$$\hat{U}(\lambda_1)\hat{U}(\lambda_2) = e^{\frac{i}{2}\cdot 0}\ \ \hat{U}\left(\lambda_1 + \lambda_2\right) \tag{A.5}$$

and the final result is

$$\hat{U}(\lambda_1)\hat{U}(\lambda_2) = \hat{U}\left(\lambda_1 + \lambda_2\right)\ . \tag{A.6}$$

2. Using (1.1) we can write

$$\hat{V}(\mu_1)\hat{V}(\mu_2) = e^{\frac{i}{2}Im\left[i\mu_1\overline{(i\mu_2)}\right]}\hat{V}\left(\mu_1 + \mu_2\right) \tag{A.7}$$

The fact that $Im\left[i\mu_1\overline{i\mu_2}\right] = Im\left[\mu_1\mu_2\right] = 0$ leads to

$$\hat{V}(\mu_1)\hat{V}(\mu_2) = e^{\frac{i}{2}\cdot 0}\ \hat{V}\left(\mu_1+\mu_2\right) \tag{A.8}$$

and the final result is

$$\hat{V}(\mu_1)\hat{V}(\mu_2) = \hat{V}\left(\mu_1+\mu_2\right)\ . \tag{A.9}$$

3. First, recall that we have

$$\hat{U}(\lambda)\hat{V}(\mu) = e^{-\frac{i}{2}\lambda\mu}\ \hat{W}\left(\zeta\right) \tag{A.10}$$

from (A.2). Then, use (1.1) in

$$\hat{V}(\mu)\hat{U}(\lambda) = e^{\frac{i}{2}Im\left[(i\frac{\mu}{d})\ \overline{\lambda d}\right]}\hat{W}\left(\zeta\right) \tag{A.11}$$

this is equal to

$$\hat{V}(\mu)\hat{U}(\lambda) = e^{\frac{i}{2}\lambda\mu}\hat{W}\left(\zeta\right) \tag{A.12}$$

or

$$\hat{W}\left(\zeta\right) = e^{-\frac{i}{2}\lambda\mu}\hat{V}(\mu)\hat{U}(\lambda) \tag{A.13}$$

inserting this into (A.10) we arrive at the desired result

$$\hat{U}(\lambda)\hat{V}(\mu) = e^{-i\lambda\mu}\hat{V}(\mu)\hat{U}(\lambda)\ . \tag{A.14}$$

- *Derivation of commutation relation of $\hat{x}$ and $\hat{V}(\mu)$:*

  First, we note that

$$[\hat{x},\hat{V}(\mu)]|x_j\rangle = \left(\hat{x}\hat{V}(\mu) - \hat{V}(\mu)\hat{x}\right)|x_j\rangle = \hat{x}\hat{V}(\mu)|x_j\rangle - \hat{V}(\mu)\hat{x}|x_j\rangle \tag{A.15}$$

Then, using equation (1.19) we obtain

$$[\hat{x},\hat{V}(\mu)]|x_j\rangle = \hat{x}|x_j-\mu\rangle - x_j\hat{V}(\mu)|x_j\rangle. \tag{A.16}$$

The action of the position operator on $|x_j-\mu\rangle$ returns $(x_j-\mu)$ and (A.16) takes the form

$$[\hat{x},\hat{V}(\mu)]|x_j\rangle = (x_j-\mu)|x_j-\mu\rangle - x_j|x_j-\mu\rangle. \tag{A.17}$$

After collecting the terms and recalling the fact that $|x_j-\mu\rangle = \hat{V}(\mu)|x_j\rangle$ for all $|x_j\rangle$ we arrive at the desired commutation relation

$$[\hat{x},\hat{V}(\mu)] = -\mu\hat{V}(\mu). \tag{A.18}$$

- *Derivation of analog of the momentum operator in Polymer framework:*

Since there is no well defined momentum operator in polymer representation in order to define an analog of the Schrödinger momentum operator, we use the standard strategy of lattice gauge theories. We first note that classically, if $k\mu$ is small then we can expand $e^{-ik\mu}$ as

$$e^{-ik\mu} = 1 - ik\mu - \frac{k^2\mu^2}{2} + \dots \tag{A.19}$$

similarly

$$e^{ik\mu} = 1 + ik\mu - \frac{k^2\mu^2}{2} + \dots \tag{A.20}$$

hence,

$$\frac{e^{-ik\mu} - e^{ik\mu}}{-2i\mu} = \frac{-2ik\mu}{-2i\mu} = k \ . \tag{A.21}$$

This means that we can define the analog of the momentum operator in a similar way. We choose a sufficiently small value μ_0 of μ and define the momentum operator on H_{poly} as $\hat{p} = \hbar\hat{K}_{\mu_0}$, where making an analogy with (A.21) and using the fact that the shift operator is represented by $\hat{V}(\mu) = e^{ik\mu}$ in Schrödinger representation we write $\hat{K}_{\mu_0}$ as

$$\hat{K}_{\mu_0} := \frac{\hat{V}(\mu_0) - \hat{V}(-\mu_0)}{2i\mu_0} \ . \tag{A.22}$$

APPENDIX B

SUPPLEMENT TO TUNNELING IN POLYMER FRAMEWORK

B.1. TRANSMISSION and REFLECTION COEFFICIENTS

When we multiply (2.78) with its complex conjugate we obtain (B.1) below.

$$|a_1|^2 \;=\; \frac{|c_1|^2 \quad f(\lambda,\varepsilon,N)}{\left(e^{2\mathrm{arccosh}(\lambda)}-1\right)^2\left(2-e^{2i\arccos(\varepsilon)}-e^{-2i\arccos(\varepsilon)}\right)} \tag{B.1}$$

From this equation it is a simple step to obtain the transmission coefficient defined as $T = \frac{|c_1|^2}{|a_1|^2}$. The final form of it is

$$T = \frac{\left(e^{2\mathrm{arccosh}(\lambda)}-1\right)^2\left(2-e^{2i\arccos(\varepsilon)}-e^{-2i\arccos(\varepsilon)}\right)}{f(\lambda,\varepsilon,N)}\,. \tag{B.2}$$

The multiple of (2.79) with its complex conjugate leads to the absolute square of a_2 which is given in (B.3).

$$|a_2|^2 \;=\; \frac{|c_1|^2 \quad g(\lambda,\varepsilon,N)}{\left(e^{2\mathrm{arccosh}(\lambda)}-1\right)^2\left(2-e^{2i\arccos(\varepsilon)}-e^{-2i\arccos(\varepsilon)}\right)} \tag{B.3}$$

Dividing (B.3) by (B.1) gives the reflection coefficient which is defined as $R = \frac{|a_2|^2}{|a_1|^2}$. The explicit form of it is

$$R = \frac{g(\lambda,\varepsilon,N)}{f(\lambda,\varepsilon,N)}\,. \tag{B.4}$$

where

$$
\begin{aligned}
f(\lambda,\varepsilon,N) = \Big(& e^{(6-2N)\operatorname{arccosh}(\lambda)} - 8e^{(5-2N)\operatorname{arccosh}(\lambda)} + 2e^{i\arccos(\varepsilon)+(5-2N)\operatorname{arccosh}(\lambda)} \\
& -12e^{i\arccos(\varepsilon)+(4-2N)\operatorname{arccosh}(\lambda)} + 4e^{2i\arccos(\varepsilon)+(2N+2)\operatorname{arccosh}(\lambda)} + 28e^{(4-2N)\operatorname{arccosh}(\lambda)} \\
& +56e^{3\operatorname{arccosh}(\lambda)} - 28e^{i\arccos(\varepsilon)+3\operatorname{arccosh}(\lambda)} - 108e^{2\operatorname{arccosh}(\lambda)} + 4e^{i\arccos(\varepsilon)+4\operatorname{arccosh}(\lambda)} \\
& -e^{2i\arccos(\varepsilon)+4\operatorname{arccosh}(\lambda)} - 4e^{2i\arccos(\varepsilon)+(3-2N)\operatorname{arccosh}(\lambda)} + 26e^{i\arccos(\varepsilon)+(3-2N)\operatorname{arccosh}(\lambda)} \\
& +33e^{(2N+2)\operatorname{arccosh}(\lambda)} - 8e^{4\operatorname{arccosh}(\lambda)} - 48e^{(3-2N)\operatorname{arccosh}(\lambda)} + 56e^{i\arccos(\varepsilon)+2\operatorname{arccosh}(\lambda)} \\
& -8e^{(2N-1)\operatorname{arccosh}(\lambda)} + 2e^{-i\arccos(\varepsilon)+(5-2N)\operatorname{arccosh}(\lambda)} - 12e^{-i\arccos(\varepsilon)+(4-2N)\operatorname{arccosh}(\lambda)} \\
& +4e^{2i\arccos(\varepsilon)+3\operatorname{arccosh}(\lambda)} + 26e^{-i\arccos(\varepsilon)+(3-2N)\operatorname{arccosh}(\lambda)} + 56e^{-i\arccos(\varepsilon)+2\operatorname{arccosh}(\lambda)} \\
& -28e^{-i\arccos(\varepsilon)+\operatorname{arccosh}(\lambda)} - 28e^{-i\arccos(\varepsilon)+3\operatorname{arccosh}(\lambda)} - 20e^{i\arccos(\varepsilon)+(2-2N)\operatorname{arccosh}(\lambda)} \\
& +e^{-2i\arccos(\varepsilon)+(4-2N)\operatorname{arccosh}(\lambda)} + 33e^{(2-2N)\operatorname{arccosh}(\lambda)} - 20e^{-i\arccos(\varepsilon)+(2-2N)\operatorname{arccosh}(\lambda)} \\
& +28e^{2N\operatorname{arccosh}(\lambda)} - 4e^{2i\arccos(\varepsilon)+2\operatorname{arccosh}(\lambda)} - 48e^{(2N+1)\operatorname{arccosh}(\lambda)} + e^{(2N-2)\operatorname{arccosh}(\lambda)} \\
& +56e^{\operatorname{arccosh}(\lambda)} - 28e^{i\arccos(\varepsilon)+\operatorname{arccosh}(\lambda)} + 4e^{-i\arccos(\varepsilon)} + 4e^{-2i\arccos(\varepsilon)+(2-2N)\operatorname{arccosh}(\lambda)} \\
& -4e^{-2i\arccos(\varepsilon)+(3-2N)\operatorname{arccosh}(\lambda)} - e^{-2i\arccos(\varepsilon)} - 4 + 26e^{-i\arccos(\varepsilon)+(2N+1)\operatorname{arccosh}(\lambda)} \\
& +4e^{-2i\arccos(\varepsilon)+\operatorname{arccosh}(\lambda)} + 4e^{2i\arccos(\varepsilon)+(2-2N)\operatorname{arccosh}(\lambda)} - 8e^{-2i\arccos(\varepsilon)+2\operatorname{arccosh}(\lambda)} \\
& -4e^{2i\arccos(\varepsilon)+(2N+1)\operatorname{arccosh}(\lambda)} + 4e^{2i\arccos(\varepsilon)+\operatorname{arccosh}(\lambda)} + 26e^{i\arccos(\varepsilon)+(2N+1)\operatorname{arccosh}(\lambda)} \\
& -12e^{i\arccos(\varepsilon)+2N\operatorname{arccosh}(\lambda)} - 4e^{2i\arccos(\varepsilon)+2\operatorname{arccosh}(\lambda)} + 2e^{-i\arccos(\varepsilon)+(2N-1)\operatorname{arccosh}(\lambda)} \\
& -12e^{-i\arccos(\varepsilon)+2N\operatorname{arccosh}(\lambda)} + 2e^{i\arccos(\varepsilon)+(2N-1)\operatorname{arccosh}(\lambda)} + e^{2i\arccos(\varepsilon)+2N\operatorname{arccosh}(\lambda)} \\
& +4e^{i\arccos(\varepsilon)} - e^{2i\arccos(\varepsilon)} - 20e^{i\arccos(\varepsilon)+(2N+2)\operatorname{arccosh}(\lambda)} + 4e^{-i\arccos(\varepsilon)+4\operatorname{arccosh}(\lambda)} \\
& +e^{-2i\arccos(\varepsilon)+2N\operatorname{arccosh}(\lambda)} - 20e^{-i\arccos(\varepsilon)+(2N+2)\operatorname{arccosh}(\lambda)} - e^{-2i\arccos(\varepsilon)+4\operatorname{arccosh}(\lambda)} \\
& +4e^{-2i\arccos(\varepsilon)+3\operatorname{arccosh}(\lambda)} - 4e^{-2i\arccos(\varepsilon)+(2N+1)\operatorname{arccosh}(\lambda)} + e^{2i\arccos(\varepsilon)+(4-2N)\operatorname{arccosh}(\lambda)} \\
& +4e^{-2i\arccos(\varepsilon)+(2N+2)\operatorname{arccosh}(\lambda)} - 4 \Big)
\end{aligned}
\tag{B.5}
$$

and

$$
\begin{aligned}
g(\lambda,\varepsilon,N) = \Big(& e^{(2N-2)\operatorname{arccosh}(\lambda)} - 48e^{(3-2N)\operatorname{arccosh}(\lambda)} - 20e^{-i\arccos(\varepsilon)+(2N+2)\operatorname{arccosh}(\lambda)} \\
& +28e^{(4-2N)\operatorname{arccosh}(\lambda)} + 56e^{3\operatorname{arccosh}(\lambda)} - 4e^{-2i\arccos(\varepsilon)+(3-2N)\operatorname{arccosh}(\lambda)} - 104e^{2\operatorname{arccosh}(\lambda)} \\
& +e^{-2i\arccos(\varepsilon)+(4-2N)\operatorname{arccosh}(\lambda)} - 10e^{-2i\arccos(\varepsilon)+2\operatorname{arccosh}(\lambda)} + 4e^{-2i\arccos(\varepsilon)+3\operatorname{arccosh}(\lambda)} \\
& -10 - 28e^{-i\arccos(\varepsilon)+3\operatorname{arccosh}(\lambda)} + 26e^{-i\arccos(\varepsilon)+(3-2N)\operatorname{arccosh}(\lambda)} + 33e^{(2-2N)\operatorname{arccosh}(\lambda)} \\
& +56e^{-i\arccos(\varepsilon)+2\operatorname{arccosh}(\lambda)} - 12e^{-i\arccos(\varepsilon)+(4-2N)\operatorname{arccosh}(\lambda)} - 28e^{-i\arccos(\varepsilon)+\operatorname{arccosh}(\lambda)} \\
& -28e^{(2N+1)\operatorname{arccosh}(\lambda)} + 56e^{\operatorname{arccosh}(\lambda)} + 2e^{-i\arccos(\varepsilon)+(5-2N)\operatorname{arccosh}(\lambda)} + 28e^{2N\operatorname{arccosh}(\lambda)} \\
& +4e^{-2i\arccos(\varepsilon)+(2-2N)\operatorname{arccosh}(\lambda)} - 20e^{-i\arccos(\varepsilon)+(2-2N)\operatorname{arccosh}(\lambda)} + 33e^{(2N+2)\operatorname{arccosh}(\lambda)} \\
& +4e^{-i\arccos(\varepsilon)+4\operatorname{arccosh}(\lambda)} + 4e^{-2i\arccos(\varepsilon)+(2N+2)\operatorname{arccosh}(\lambda)} + 4e^{-2i\arccos(\varepsilon)+\operatorname{arccosh}(\lambda)} \\
& +e^{-2i\arccos(\varepsilon)+2N\operatorname{arccosh}(\lambda)} + 4e^{i\arccos(\varepsilon)+4\operatorname{arccosh}(\lambda)} + 26e^{-i\arccos(\varepsilon)+(2N+1)\operatorname{arccosh}(\lambda)} \\
& +4e^{2i\arccos(\varepsilon)+3\operatorname{arccosh}(\lambda)} + e^{2i\arccos(\varepsilon)+(4-2N)\operatorname{arccosh}(\lambda)} - 12e^{-i\arccos(\varepsilon)+2N\operatorname{arccosh}(\lambda)} \\
& -10e^{2i\arccos(\varepsilon)+2\operatorname{arccosh}(\lambda)} + 26e^{i\arccos(\varepsilon)+(3-2N)\operatorname{arccosh}(\lambda)} - 28e^{i\arccos(\varepsilon)+3\operatorname{arccosh}(\lambda)} \\
& +2e^{i\arccos(\varepsilon)+(5-2N)\operatorname{arccosh}(\lambda)} - 12e^{i\arccos(\varepsilon)+(4-2N)\operatorname{arccosh}(\lambda)} + 56e^{i\arccos(\varepsilon)+2\operatorname{arccosh}(\lambda)} \\
& -20e^{i\arccos(\varepsilon)+(2-2N)\operatorname{arccosh}(\lambda)} + 4e^{2i\arccos(\varepsilon)+(2-2N)\operatorname{arccosh}(\lambda)} + 4e^{2i\arccos(\varepsilon)+\operatorname{arccosh}(\lambda)} \\
& -28e^{i\arccos(\varepsilon)+\operatorname{arccosh}(\lambda)} + 4e^{i\arccos(\varepsilon)} + 4e^{2i\arccos(\varepsilon)+(2N+2)\operatorname{arccosh}(\lambda)} + 4e^{-i\arccos(\varepsilon)} \\
& +e^{2i\arccos(\varepsilon)+2N\operatorname{arccosh}(\lambda)} - 20e^{i\arccos(\varepsilon)+(2N+2)\operatorname{arccosh}(\lambda)} + 2e^{-i\arccos(\varepsilon)+(2N-1)\operatorname{arccosh}(\lambda)} \\
& -4e^{2i\arccos(\varepsilon)+(2N+1)\operatorname{arccosh}(\lambda)} - 12e^{i\arccos(\varepsilon)+2N\operatorname{arccosh}(\lambda)} + 2e^{i\arccos(\varepsilon)+(2N-1)\operatorname{arccosh}(\lambda)} \\
& -8e^{(5-2N)\operatorname{arccosh}(\lambda)} - 8e^{(2N-1)\operatorname{arccosh}(\lambda)} + e^{(6-2N)\operatorname{arccosh}(\lambda)} - 20e^{(2N+1)\operatorname{arccosh}(\lambda)} \\
& -4e^{-2i\arccos(\varepsilon)+(2N+1)\operatorname{arccosh}(\lambda)} - 10e^{4\operatorname{arccosh}(\lambda)} - 4e^{2i\arccos(\varepsilon)+(3-2N)\operatorname{arccosh}(\lambda)} \\
& +26e^{i\arccos(\varepsilon)+(2N+1)\operatorname{arccosh}(\lambda)} \Big) .
\end{aligned}
\tag{B.6}
$$